Article

Coupling Advanced Geo-Environmental Indices for the Evaluation of Groundwater Quality: A Case Study in NE Peloponnese, Greece

Panagiotis Papazotos [1,2,*], Maria Vlachomitrou [3], Despoina Psarraki [1], Eleni Vasileiou [1] and Maria Perraki [1]

[1] School of Mining and Metallurgical Engineering, Division of Geo-Sciences, National Technical University of Athens, 9 Heroon Polytechniou St., 15773 Zografou, Greece

[2] School of Engineering, Department of Mineral Resources Engineering, University of Western Macedonia, 50100 Kozani, Greece

[3] Faculty of Geology and Geoenvironment, National and Kapodistrian University of Athens, Panepistimiopolis, Zografou, 15784 Athens, Greece

[*] Correspondence: papazotos@metal.ntua.gr; Tel.: +30-2107722059

Abstract: Water and its management have played a pivotal role in the evolution of organisms and civilizations, fulfilling essential roles in personal use, industry, irrigation, and drinking from ancient times to the present. This study seeks to evaluate groundwater quality for irrigation and drinking in the Northern Peloponnese region, specifically the wells of Loutraki and Schinos areas and the springs of the Gerania Mountains (Mts.), using geo-environmental indices and ionic ratios. For the first time, geo-environmental indices have been applied to a region where groundwater serves multiple purposes, addressing the challenge of understanding their dynamics to optimize their application in environmental science and groundwater pollution research. To achieve this, 68 groundwater samples from the study area were utilized, and a total of 25 geo-environmental indices were calculated to assess water quality. These indices examined: (i) drinking suitability (NPI, RI, PIG, WQI, and WPI), (ii) irrigation suitability (SAR, KR, %Na, PS, MAR, RSC, SSP, TH, PI, IWQI, and TDS), (iii) potentially toxic element (PTE) loadings (Cd, HEI, and HPI), and (iv) major hydrogeochemical processes, expressed as ionic ratios (Ca/Mg, Ca/SO_4, Ca/Na, Cl/NO_3, Cl/HCO_3, and Si/NO_3). Data processing involved descriptive statistics, hydrogeochemical bivariate plots, Spearman correlation coefficients, and multivariate statistical analyses, including factor analysis (FA) and R-mode hierarchical cluster analysis (HCA). Results revealed that all groundwater samples (100%) from the Loutraki area and the Gerania Mts. were of good quality for both drinking and irrigation purposes. In contrast, groundwater from the Schinos area exhibited lower quality, with most samples (93.9%) considered suitable only for irrigation. The deterioration in the coastal aquifer of the Schinos area is attributed to elevated concentrations of Cl^-, Na^+, NO_3^-, As, and Cr resulting from salinization and relatively limited anthropogenic influences. The study highlights that relying on individual geo-environmental indices can yield misleading results due to their dependence on factors such as researcher expertise, methodological choices, and the indices' inherent limitations. Consequently, this research emphasizes the necessity of combining indices to enhance the reliability, accuracy, and robustness of groundwater quality assessments and hydrogeochemical evaluations. Last but not least, the findings demonstrate that calculating all available geo-environmental indices is unnecessary. Instead, selecting a subset of indices that either reflect the impact of specific elemental concentrations or can be effectively integrated with others is sufficient. This streamlined approach addresses challenges in optimizing geo-environmental index applications and contributes to improved groundwater resource management.

1. Introduction

Groundwater is a crucial resource for various human activities, playing a vital role in agriculture, industry, and domestic water supply [1,2]. It serves as the primary source of irrigation for crops, especially in regions with limited surface water availability, ensuring food security [3]. Industries rely on groundwater for processes such as cooling, cleaning, and manufacturing, while it also provides drinking water for millions of people worldwide [4,5]. Effective groundwater management is essential to prevent over-extraction, contamination, depletion, scarcity, and stress [6–8]. This includes practices like monitoring water levels, implementing sustainable withdrawal limits, protecting recharge areas, and promoting water conservation and groundwater sustainability to maintain its availability for future generations [2,9].

To date, research on groundwater resource quality has primarily concentrated on identifying the origins of dissolved solutes and other chemical elements, distinguishing between geogenic and anthropogenic sources. Many studies have employed statistical methods and geographic information system (GIS) tools (e.g., [10–13], along with advanced techniques such as machine learning (ML) algorithms [14–16] and spatial autocorrelation [17–19]. These combined methods have been used to analyze key factors influencing water quality. Additionally, several studies have utilized various geo-environmental indices (the term 'geo-environmental indices' is defined in this study as all indices assessing water quality status) to evaluate the chemical suitability of water for specific uses [20–22]. While these geo-environmental indices have been applied in numerous studies worldwide [14,22–24], their application in groundwater quality assessments in Greece remains limited and is mentioned only in a few case studies [25–27]. However, no comprehensive evaluation of these geo-environmental indices has been conducted to highlight their strengths and weaknesses within a specific case study. The lack of such thorough investigations may lead to potentially erroneous or misleading conclusions, indicating that the assessment of water quality through these methodologies is still incomplete. Therefore, it is crucial to explore the optimal application of geo-environmental indices in areas where (i) water quality data are available and (ii) groundwater resources are used for various purposes. Therefore, a study that draws informed conclusions regarding the effective use of these indices in a study area—while clearly identifying their weaknesses, issues, shortcomings, and poor practices—is highly important.

The Loutraki–Schinos–Gerania Mountains (Mts.) region has been extensively studied by various Greek research institutions, including the National Technical University of Athens (NTUA), the National Kapodistrian University of Athens (NKUA), and the Hellenic Survey of Geology and Mineral Exploration (HSGME), as well as by numerous researchers. This attention is due to the region's significant geological, mineralogical, and hydrogeological features, alongside concerns related to groundwater quality. Papadopoulos and Lappas [28] were first to identify elevated levels of chromium (Cr), hexavalent chromium [Cr(VI)], and nitrate (NO$_3$−) in the coastal alluvial aquifer of the Schinos area. Subsequent research by Pyrgaki et al. [29] confirmed elevated groundwater concentrations of these contaminants in the Loutraki, Schinos, and Gerania Mts. areas. Papazotos et al. [30] further established a statistical relationship between Cr, Cr(VI), and NO$_3$− concentrations, and also reported increased levels of arsenic (As) in the groundwater. Both Papazotos et al. [30] and Pyrgaki et al. [31] emphasized the geogenic origin of Cr in the Loutraki area, attributing

it to the ultramafic rocks of the Gerania Mts. Additionally, Kelepertzis et al. [32] and Pyrgaki et al. [33] conducted isotopic analyses using $\delta^{18}O_{NO3}$ and $\delta^{15}N_{NO3}$ in the Schinos area, suggesting that the likely sources of NO_{3-} in the groundwater are septic tanks and nitrogen (N)-bearing fertilizers; this fact supports the findings of Papazotos et al. [30], confirming the hydrogeochemical findings about the role of the nitrogen (N) cycle in the mobilization of potentially toxic elements (PTEs) in the groundwater resources. To date, there remains a research gap regarding the suitability of groundwater resources for various uses based on their quality. A water suitability study is therefore necessary for this area; calculating geo-environmental indices could offer valuable insights into optimal water use and management by uncovering hidden hydrogeochemical properties.

This study aims to assess the groundwater quality in Northern Peloponnese, specifically in the broader area of Loutraki–Schinos–Gerania Mts., for various uses including drinking, irrigation, and evaluating PTE loads. The assessment employs geo-environmental indices and ionic ratios, contributing to the fields of environmental geochemistry, hydrogeology, and groundwater resource management. In this research, we calculated geo-environmental indices: (i) to determine the suitability of irrigation water, (ii) to assess the suitability of drinking water, (iii) to evaluate PTE loads, (iv) to compare values across three different subcases, and (v) to conduct a comprehensive evaluation to ensure the holistic, safe, and sustainable use of water. The significance of this paper lies in the application of chemical analyses and the subsequent calculation of geo-environmental indices to evaluate water suitability using mathematical equations. This is particularly important in the Northern Peloponnese, where groundwater resources serve both drinking and irrigation needs. For the first time, geo-environmental indices have been calculated for an area where groundwater is used for multiple purposes. This approach ensures efficient groundwater management, protects human health, and optimizes water demand.

2. Materials and Methods

2.1. Description of the Study Area

The study area is located in the Corinth prefecture of the NE Peloponnese, Greece, between latitudes 37°56′00″ N and 38°04′00″ N and longitudes 22°57′00″ E and 23°08′00″ E; it encompasses Loutraki Town, the Gerania Mts., and Schinos Village. Elevations were recorded up to 90 m in the Schinos area, up to 190 m in the Loutraki area, and up to 1351 m in the Gerania Mts. A simplified lithological map showing the groundwater sampling sites for the three subareas (i.e., wells in Loutraki, Gerania springs, and wells in Schinos) is presented in Figure 1.
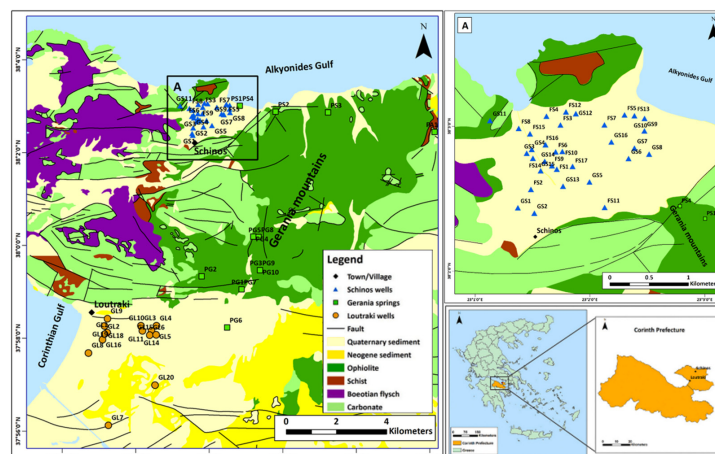
Figure 1. A simplified geological map of the study area [34,35] with the groundwater sampling sites. An enlarged image of the Schinos area is given in (A) [30].

The area's geological and hydrogeological characteristics significantly influence groundwater quality. In Schinos, located in the Northern Corinth prefecture, dominant formations include Triassic–Jurassic carbonate rocks (limestones), Upper Jurassic–Lower Cretaceous Boeotian flysch, Lower Cretaceous ophiolites, and Quaternary sediments [36]. The aquifer systems here consist of a karstic aquifer in the south and west, a fractured ultramafic aquifer in the south and SE, and a granular alluvial unconfined coastal aquifer in the central part. The main focus is on the alluvial aquifer, composed of sands, gravels, and conglomerates, recharged by lateral inflows, karstic aquifer inflows, and direct precipitation infiltration [37]. The vadose zone in the Schinos area reaches up to 15 m, with piezometric elevations ranging from −0.9 to 10.2 m [38]. The local economy is driven by tourism and, to a lesser extent, agriculture and livestock.

In Loutraki, geological formations include Lower Cretaceous ophiolites, Triassic–Jurassic carbonate rocks, Neogene marls, and Quaternary sediments. Aquifer systems include a karstic aquifer in the north and west, a fractured ultramafic aquifer in the northwest, and a major unconfined alluvial aquifer. This aquifer is recharged by precipitation, surface runoff infiltration, and lateral inflows. Its vadose zone thickness varies from 40 m in the east to over 100 m in the west [39]. Hydraulic disconnection is maintained by intercalating marls. Loutraki's thermal springs, linked to the karstic aquifer, are influenced by the South Aegean volcanic arc, with a probable deep geothermal reservoir at 80 °C [40]. Furthermore, it is noted that approximately 10 km from Loutraki Town lies the inactive Sousaki volcano, hosting a geothermal reservoir and characterized by an active hydrothermal activity with low-temperature gas emissions that have extensively altered the surrounding rocks [41].

The Gerania Mts., forming the northern part of the Corinth prefecture, include sedimentary and volcanic rocks, Triassic–Jurassic carbonate rocks, Upper Jurassic radiolarian sediments, Upper Jurassic–Lower Cretaceous Boeotian flysch, and Lower Cretaceous ultramafic rocks (mainly peridotite and serpentinite) [35,42]. The area is tectonically active, characterized by normal faults and steep slopes, which enhance the development of a highly permeable carbonate aquifer and semi-permeable fractured ultramafic spring systems [39]. The degree of weathering in peridotite is more pronounced along the fault zones. The dominant lithology is spinel lherzolite, with local occurrences of dunite and gabbro. It is worth noting that magnesite and other carbonate minerals are commonly found along fractured zones. Furthermore, the surface water network is dendritic in structure, consisting of two primary streams.

The study area is geodynamically situated within the complex neotectonics of the Gulf of Corinth, one of the most tectonically active regions in Greece, marked by significant seismic activity. The geological structure of central mainland Greece, including the Gulf of Corinth, is predominantly controlled by a series of E–W to NW–SE-trending normal faults, which have played a key role in shaping the region's topography [43,44]. Along the southern margin of the Gulf of Corinth, a set of prominent normal faults, ranging in length from 15 to 25 km, exhibit a strike of approximately N100° and dip northward at angles of about 50°. The SE lowland region of the Loutraki area is part of the eastern Corinthian graben, while the mountainous region corresponds to the Gerania tectonic horst [43,44].

Taking into account demographic data, the Municipality of Corinth spans a total area of 611.02 Km² and, according to the 2021 census conducted by the Hellenic Statistical Authority [45], has a population of 55,941, resulting in a population density of 91.55 inhabitants per Km². The population in the study area exerts pressure on the groundwater resources, which serve multiple purposes. In the Loutraki area, wells primarily supply drinking water, while in the Schinos area, groundwater is mainly used for irrigation. The region is a popular summer destination, attracting significant tourism and driving increased water demand

during the warmer months. It experiences a typical Mediterranean climate, classified as Csa (hot-summer Mediterranean) under Köppen's classification, characterized by mild, wet winters and hot, dry summers with sharply reduced precipitation in the summer months. According to the Hellenic National Meteorological Service (HNMS), 33 years of data (1988–2010), from the Velo Corinthia meteorological station [46] indicate that the highest average monthly temperature is observed in July (28.7 °C), while the lowest occurs in January (9.1 °C), with the mean temperature being closer to the average maximum temperature. Precipitation peaks in December at 78.6 mm and drops to its lowest in July, averaging 5 mm. The wet season spans from October to mid-March, while the dry season extends from mid-March to mid-October.

According to the Corine Land Cover (CLC) 2018 data [47], the Prefecture of Corinth comprises four main land-use categories. Forest and semi-natural areas dominate, covering 68.4% of the region, followed by agricultural areas at 21.8%, artificial surfaces at 5.8%, and water bodies at 3.9%. These land uses are classified into four distinct categories: (i) forest and seminatural areas (coniferous forests, natural grasslands, sclerophyllous vegetation, and transitional woodland shrubs), (ii) agricultural areas (non-irrigated arable land, fruit trees and berry plantations, olive groves, pastures, complex cultivation patterns, and land primarily occupied by agriculture), (iii) artificial surfaces (continuous and discontinuous urban fabrics, commercial or industrial units, road and rail networks and associated land, and sport and leisure facilities), and (iv) water bodies (marine waters).

2.2. Sampling and Analysis

A total of 68 groundwater samples were collected from the study area: (i) 33 from irrigation wells in the Schinos area, (ii) 15 from Gerania springs, and (iii) 20 from drinking and irrigation wells in the Loutraki area. Sampling occurred during two campaigns in November 2016 and June 2017. Well samples were collected after purging residual water for at least 15 min, while spring samples were obtained via natural discharge. Water was collected in pre-cleaned 1000 mL polyethylene bottles, which were rinsed with sample water before collection. Samples were divided into three subsamples: 500 mL for major cations (Ca^{2+}, Mg^{2+}, Na^+, K^+) and anions (Cl^-, SO_4^{2-}, HCO_3^-, NO_3^-, PO_4^{3-}) 100 mL for PTEs and other trace elements (e.g., As, Cd, Cr, Ni, Si, Pb, Zn, etc.); and 25 mL for Cr(VI). Physical parameters such as electrical conductivity (EC), dissolved oxygen (DO), pH, and oxidation–redox potential (ORP/Eh) were measured in situ using a YSI Professional Digital Sampling System (ProDSS). Samples were stored in a cooler and refrigerated at 4 °C prior to analysis. The 500-mL subsamples were filtered and analyzed within 8 h to determine the dissolved forms of major ions. Major ions were determined using atomic absorption spectrometry (AAS), titration, spectrophotometry, or turbidimetry, while PTEs, other trace elements, and Cr(VI) were measured by inductively coupled plasma mass spectrometry (ICP-MS). All analyses followed international quality control protocols—using blanks, standards, and duplicate samples to maintain charge balance errors within ±10%—and were conducted in an ISO/IEC 17025:2005 (UNE-EN ISO/IEC/17025:2005, 2005 [48]. General Requirements for the Competence of Testing and Calibration Laboratories) certified laboratory, ensuring high precision, accuracy, and reliability. The data of this study were previously published in our earlier research [30], which also provides detailed information on the sampling and analysis procedures.

2.3. Data Treatment

This section includes the calculation of geo-environmental indices with equations that utilize the results of chemical determinations and the statistical treatment of various variables.

2.3.1. Evaluation of Water Quality for Various Purposes

The suitability of water is directly related to its intended use. Numerous geo-environmental indices are available to evaluate water quality for different purposes; several of those used in this study are shown in Figure 2. In general, these indices offer valuable information on water suitability (e.g., for drinking or irrigation), water quality assessment (e.g., PTEs and other major/minor elements), and the identification of key hydrogeochemical processes (e.g., contributions from geological formations, anthropogenic activities, and geochemical reactions) (Figure 2).
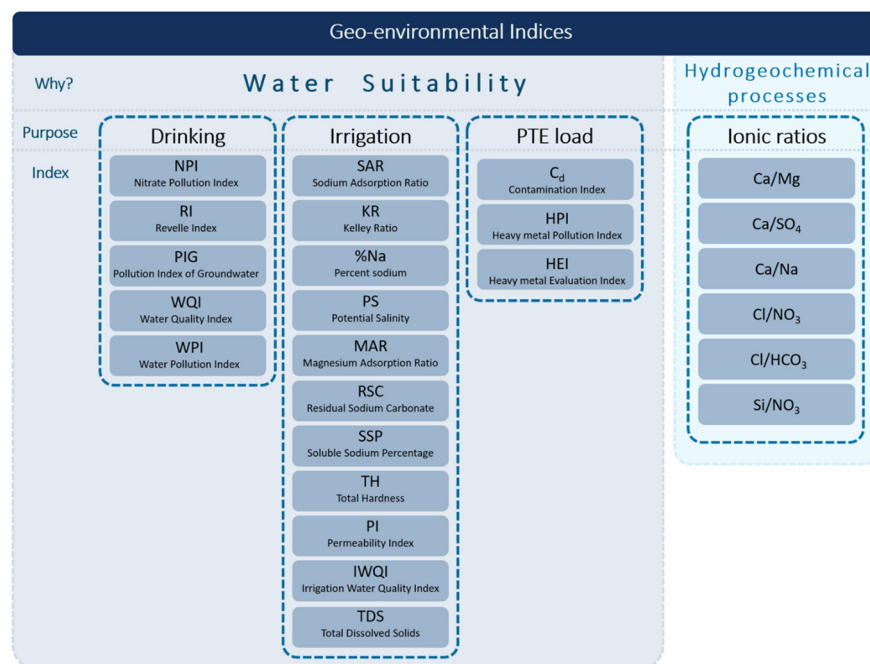

Figure 2. Classification of the 25 calculated geo-environmental indices of this study.

Drinking

This section includes the calculation of geo-environmental indices with equations that utilize the results of chemical determinations and the statistical treatment of various variables.

The evaluation of groundwater quality for drinking purposes was conducted using the following five geo-environmental indices: nitrate pollution index (NPI), Revelle index (RI), pollution index of groundwater (PIG), water quality index (WQI), and water pollution index (WPI). Detailed descriptions and information for each index are provided below:

Nitrate pollution index (NPI): The NPI is a single parameter water quality index that is used to calculate NO_3^- contamination. The NPI shows that human activity has contributed to NO_3^- pollution in groundwater. To calculate NPI, Equation (1) was used [49]:

$$NPI = \frac{C_s - HAV}{HAV} \tag{1}$$

where C_s represents the NO_3^- concentration in each groundwater sample, while HAV (human-affected value) refers to the threshold level of NO_3^- in groundwater, set at 10 mg/L according to Panno et al. [50]. Based on NPI values, water quality was classified into five categories: (a) clean water (NPI < 0), (b) lightly polluted water (NPI: 0–1), (c) moderately polluted water (NPI: 1–2), (d) significantly polluted water (NPI: 2–3), and (e) very significantly polluted water (NPI > 3).

Revelle index (RI): The RI was used to assess groundwater salinity in the study area. It was calculated using Equation (2) [51], with all ion concentrations expressed in meq/L:

$$RI = \frac{Cl^-}{HCO_3^- + CO_3^{2-}} \tag{2}$$

Based on RI values, water quality was classified into three categories: (a) unaffected (RI < 0.5), (b) slightly affected (RI = 0.5–6.6), and (c) strongly affected (RI > 6.6) by salinity. In general, RI values below 1 suggest good water quality.

Pollution index of groundwater (PIG): The PIG was calculated following the method proposed by Subba Rao [52], which evaluates the relative influence of individual chemical parameters (i.e., pH, TDS, TH, Ca^{2+}, Mg^{2+}, Na^+, K^+, HCO_{3-}, SO_4^{2-}, Cl^-, and NO_{3-}). The computation of the PIG involved a total of five steps:

○ Step I: Assigning relative weights (R_w): Each chemical parameter was assigned a relative weight on a scale from 1 to 5, reflecting its impact on human health. Potassium (K^+) received the minimum weight of 1, while TDS, SO_4^{2-}, and NO_{3-} were assigned the maximum weight of 5 [52].

○ Step II: Calculating weight parameters (W_p): The weight parameter for each chemical was calculated to assess its contribution to overall groundwater quality, using Equation (3):

$$W_p = \frac{R_w}{\sum R_w} \tag{3}$$

○ Step III: Determining status of concentration (S_c): The concentration status for each parameter was established by dividing the concentration (C) of the parameter in each sample by its corresponding drinking water quality standard limit (D_s) (Equation (4)):

$$S_c = \frac{C}{D_s} \tag{4}$$

○ Step IV: Calculating overall groundwater quality (O_w): The overall groundwater quality was calculated by multiplying the weight parameter (W_p) with the concentration status (S_c) (Equation (5)):

$$O_w = W_p \times S_c \tag{5}$$

○ Step V: Calculating PIG: Finally, the PIG was obtained by summing all values of O_w (Equation (6)), providing a comprehensive assessment of pollution's impact on the groundwater system.

$$PIG = \sum O_w \tag{6}$$

○ Based on the calculated PIG values, the water pollution status was classified into five categories: (a) no significant pollution (PIG < 1.0), (b) low pollution (PIG = 1.0–1.5), (c) moderate pollution (PIG = 1.5–2.0), (d) high pollution (PIG = 2.0–2.5), and (e) very high pollution (PIG > 2.5).

Water quality index (WQI): The WQI, as defined by Horton [53] and Brown et al. [54], utilizes the same relative weights assigned to each chemical parameter in the PIG, as outlined in Equation (3) using a total of 9 parameters (TDS, Ca^{2+}, Mg^{2+}, Na^+, K^+, HCO_{3-}, SO_4^{2-}, Cl^-, and NO_{3-}). The quality rating scale (q_i) for each parameter is calculated by dividing its concentration in each water sample by the corresponding standard, then multiplying the result by 100 as shown in the following Equation (7).

$$q_i = S_c \times 100 \tag{7}$$

To compute the final stage of the WQI, the SI for each chemical parameter (SI_i) is determined using Equation (8).

$$SI_i = W_p \times q_i \tag{8}$$

The WQI is then calculated by summing all the SI values, as expressed in Equation (9):

$$WQI = \sum SI_i \tag{9}$$

Based on the calculated WQI values, water quality levels are classified into five categories: (a) excellent water (WQI < 50), (b) good water (WQI = 50–100), (c) poor water (WQI = 100–200), (d) very poor water (WQI = 200–300), and (e) unsuitable for drinking (WQI > 300).

Water pollution index (WPI): The WPI offers a flexible and rational alternative approach to existing indexing systems by consolidating multiple chemical variables into a single value index [55]. This method employs a total of ten water quality parameters (pH, EC, Ca^{2+}, Mg^{2+}, Na^+, K^+, HCO_{3-}, $SO_4{}^{2-}$, Cl^-, and NO_{3-}) for calculating WPI. The calculation involves two steps. The first step is to compute the pollution load (PL_i) (Equation (10)):

$$PL_i = 1 + \frac{C_i - S_i}{S_i} \tag{10}$$

where PLi represents the pollution load, C_i is the observed ionic concentration, and S_i is the highest desirable limit prescribed for drinking water quality.

The PL_i depends on pH. If the pH is <7, the PL_i is computed using Equation (11):

$$PL_i = 1 + \frac{C_i - 7}{S_a - 7} \tag{11}$$

where S_a is the lowest desirable limit of pH (6.5) recommended for drinking water quality. If the pH is >7, PL_i is calculated using Equation (12):

$$PL_i = 1 + \frac{C_i - 7}{S_b - 7} \tag{12}$$

where S_b is the maximum desirable limit of pH (8.5) for drinking water quality.
In the second step, WPI is determined by averaging the PLi using Equation (13):

$$WPI = \frac{1}{n} \sum_{i=1}^{n} PL_i \tag{13}$$

where *n* is the number of chemical variables.
The WPI values can be classified into four categories: (a) excellent water (WPI < 0.5), (b) good water (WPI = 0.5–0.75), (c) moderately polluted water (WPI = 0.75–1.0), and (d) highly polluted water (WPI: >1.0).

Irrigation

The assessment of groundwater quality for drinking purposes was conducted using 11 geo-environmental indices: SAR, KR, %Na, PS, MAR, RSC, SSP, TH, PI, IWQI, and TDS. A detailed explanation of each index, including key information, is provided below:

Sodium adsorption ratio (SAR): The SAR is a significant irrigation quality index that points out Na^+ hazard and evaluates the cations concentrations expressed in meq/L according to Equation (14) [56]:

$$SAR = \frac{Na^+}{\sqrt{\frac{(Ca^{2+}+Mg^{2+})}{2}}} \times 100 \tag{14}$$

Excessive Na^+ concentration in irrigation water can reduce soil permeability by altering its structure. Significant changes in Na^+ concentrations in irrigation water often lead to modifications in soil composition. When water contains high levels of both Na^+ and Ca^{2+}, ion exchange occurs, causing the soil to become saturated with Na^+ and depleted of Ca^{2+}; this imbalance negatively affects soil quality and reduces crop yields [57]. The classification of SAR values includes four categories: (a) excellent (SAR < 10), (b) good (SAR = 10–18), (c) doubtful—unsuitable for most crops due to elevated sodium levels (SAR = 18–26), and (d) unsuitable—unsatisfactory for all crops due to very high Na^+ levels (SAR > 26).

Kelley ratio (KR): The KR is a method used to assess the impact of Na^+ on water quality, particularly for irrigation purposes. It evaluates Na^+ levels in relation to alkaline earth (i.e., Ca^{2+} and Mg^{2+}) concentrations in groundwater, as proposed by Kelley [58,59]. Water is considered unsuitable for irrigation if the Na^+ content exceeds the concentration of alkaline earths in groundwater. Finally, KR is determined using Equation (15) [58,59]:

$$KR = \frac{Na^+}{Ca^{2+} + Mg^{2+}} \tag{15}$$

A KR value greater than 1 indicates excess Na^+ and is not recommended for irrigation due to alkali hazards, while water with a KR value less than 1 is suitable for irrigation [58].

Percent sodium (%Na): %Na concentration is a factor to assess its suitability for irrigation purposes [60]. The Na^+ concentration is vital for classifying irrigation water, as it bonds with soil particles, reducing water movement [61]. Sodium ions (Na^+) form alkaline soils with CO_3^{2-} and saline soils with chloride, both inhibiting crop growth [57]. High Na^+ levels in irrigation water cause a base-exchange reaction, replacing Ca^{2+} and Mg^{2+} ions, further limiting water movement. This results in compacted soils that restrict air and water flow, especially in wet conditions [62]. The %Na values are calculated using Equation (16) [60]:

$$\%Na = \frac{Na^+}{Ca^{2+} + Mg^{2+}+Na^+ + K^+} \times 100 \tag{16}$$

The classification of water is based on %Na as excellent (<20%), good (20–40), permissible (40–60), doubtful (60–80), and unsuitable (>80%).

Potential salinity (PS): To assess the salinity of the groundwater, the PS index—another indicator of irrigation quality—was calculated based on Cl^- and SO_4^{2-} concentrations. A high Cl^-/SO_4^{2-} ratio can lead to scale formation in irrigation systems, which may affect water distribution to crops [63,64]. The PS index, expressed in meq/L, is determined using Equation (17) as follows:

$$PS = Cl^- + \frac{SO_4^{2-}}{2} \tag{17}$$

A PS value greater than 3 indicates unsafe water quality for irrigation, while a value less than 3 signifies safe water quality [65].

Magnesium adsorption ratio (MAR): The MAR index, developed by Szabolcs and Darab [66], is used to assess Mg hazards, as Mg increases soil alkalinity, thereby degrading soil quality and crop yields [23,67]. This index operates on the principle that Ca^{2+} and Mg^{2+}

ions are typically in equilibrium in most groundwater [68,69]. Equation (18) was used to calculate the MAR index:

$$MAR = \frac{Mg^{2+}}{Ca^{2+} + Mg^{2+}} \times 100 \tag{18}$$

Groundwater is considered suitable for irrigation when the MAR value is below 50, but it becomes harmful and unsuitable when the MAR value exceeds 50.

Residual sodium carbonate (RSC): In alkaline water, the high concentration of HCO_3^- increases the likelihood of Ca^{2+} and Mg^{2+} precipitating as carbonates, especially when compared to water with lower HCO_3^- levels. To quantify this effect, ionic concentrations are measured in meq/L, and an index known as RSC is used [70]. Essentially, RSC provides an additional metric for determining whether water is suitable for irrigation, and it is represented by Equation (19) [70]:

$$RSC = (HCO_3^- + CO_3^{2-}) - (Ca^{2+} + Mg^{2+}) \tag{19}$$

RSC values can categorize water quality into three classes: (a) good (RSC < 1.25), (b) moderate (RSC = 1.25–2.50), and (c) unsuitable (RSC > 2.50).

Soluble sodium percentage (SSP): The SSP represents the ratio of Na and K ions to the total cation concentration and is used to assess irrigation water quality, particularly concerning Na^+ hazards. High Na^+ levels, as noted above, can reduce soil permeability and inhibit plant growth. SSP was calculated using Equation (20) from Todd [57], with ionic concentrations expressed in meq/L:

$$SSP = \frac{Na^+ + K^+}{Ca^{2+} + Mg^{2+} + Na^+ + K^+} \times 100 \tag{20}$$

Groundwater is considered suitable for irrigation when the SSP value is below 50, but it is unsuitable when the SSP value exceeds 50.

Total hardness (TH): TH is primarily influenced by the concentrations of Mg^{2+} and Ca^{2+} in water [71], both of which are essential for human health. However, high TH levels in drinking water are associated with various health issues, including arterial calcification, urinary stones, kidney and bladder disorders, and digestive problems [72]. TH was calculated in mg/L by means of Equation (21) [57]:

$$TH = 2.497Ca^{2+} + 4.11Mg^{2+} \tag{21}$$

Based on TH values, water was classified into four categories: (a) soft water (TH < 60 mg/L), (b) moderately hard water (TH = 60–120 mg/L), (c) hard water (TH = 120–180 mg/L), and (d) very hard water (TH > 180 mg/L) [73].

Permeability index (PI): PI is used to assess and classify the quality of irrigation water. Long-term irrigation can impact soil permeability, which is influenced by the concentrations of Na^+, Ca^{2+}, Mg^{2+}, and HCO_3^- in the soil. Doneen [63,64] proposed Equation (22) (with all ion concentrations expressed in meq/L) to calculate PI:

$$PI = \frac{Na^+ + \sqrt{HCO_3^-}}{Ca^{2+} + Mg^{2+} + Na^+} \times 100 \tag{22}$$

PI values can be categorized into three classes: (a) class I—suitable for irrigation (PI > 75%), (b) class II—good for irrigation (PI = 25–75%), and (c) class III—unsuitable for irrigation (PI < 25%).

Irrigation water quality index (IWQI): IWQI was calculated based on five key water quality parameters: EC, SAR, Na^+, Cl^-, and HCO_3^- following the methodology of

Meireles et al. [74]. First, the concentration units of the water samples were converted from mg/L to meq/L. In this section, the IQWI was assessed by calculating the water quality parameter values (q_i) and the cumulative weight (W_i). Table 1 summarizes the irrigation water quality parameters and their proposed limiting values [74]. The q_i values for the five water quality parameters (qEC, qSAR, qNa$^+$, qCl$^-$, and qHCO$_3$-) were determined using Equation (23). The upper limits of the parameter ranges indicated in Table 1 were used as the highest value of the observed sample values to evaluate x_{imap}.

$$IWQI = Q_{max} - \left(\frac{\left(x_{ij} - x_{inf} \right) \times q_{imap}}{x_{amp}} \right) \qquad (23)$$

where Q_{max} is the upper value of the q_i class of, X_{ij} represents the observed values for each parameter (Table 1), X_{inf} is the lower limit of the class to which the observed parameter belongs, q_{imap} represents the class amplitude for qi classes, and x_{imap} corresponds to class amplitude for the specific parameter.

Table 1. Parameter-limiting values of IWQI for quality measurement (q_i) calculation [74].

q_i	EC (µS/cm)	SAR (meq/L)$^{1/2}$	Na$^+$ (meq/L)	Cl$^-$ (meq/L)	HCO$_3$$^-$ (meq/L)
85–100	200–750	<3	2–3	<4	1–1.5
60–85	750–1500	3–6	3–6	4–7	1.5–4.5
35–60	1500–3000	6–12	6–9	7–10	4.5–8.5
0–35	<200 or >3000	>12	<2 or >9	>10	<1 or >8.5

Finally, the overall IWQI was determined using Equation (24):

$$IWQI = \sum_{1}^{n} q_i w_i \qquad (24)$$

where *n* is the number of parameters (in this case a total of 5 parameters); q_i values from Table 1 are multiplied by the corresponding weight (w_i) of each parameter, as listed in Table 2 [74]. It is important to note that, in calculating the final IWQI value, we applied four classification categories of limiting values for the five parameters (Table 1), following the methodological framework outlined by Meireles et al. [70], and incorporating the five distinct categories of restrictions and recommendations for water usage presented in Table 3.

Table 2. The weights of the IWQI parameters [74].

Parameters	Wi
EC	0.211
Na$^+$	0.204
HCO$_3$$^-$	0.202
Cl$^-$	0.194
SAR	0.189
Total	1.000

Total dissolved solids (TDS): TDS measures the total amount of dissolved solids in the groundwater, expressed in mg/L; TDS is a crucial measure for determining the presence and concentration of pollutants. Generally, TDS indicates the amount of dissolved salts in irrigation water, with higher levels reducing a plant's ability to absorb nutrients efficiently due to increased salinity [75]. TDS value was computed by adding the major cations and anions determined in each of the water samples, as indicated by the following equation (Equation (25)):

$$TDS = \sum Major\ cations + \sum Major\ anions \qquad (25)$$

TDS values > 500 mg/L are considered the highest desirable limits according to the World Health Organization (WHO) [76]. While TDS is often used as a general water quality index, in this study, it is specifically treated as an irrigation suitability index due to its significant impact on agricultural water use, particularly in areas with high salinity. In the context of this study, which is located near the sea, high TDS levels in groundwater can affect irrigation practices. Although high TDS levels (up to 1500 mg/L) are generally not harmful to humans [77], they can adversely affect living organisms, causing major cardiovascular and renal disorders [78].

Table 3. IWQI characteristics [74].

IWQI	Water Use Restriction	Recommendation	
		Soil	**Plant**
85–100	No restriction (NR)	Suitable for most soils, with a low likelihood of causing salinity or sodicity issues. Leaching is recommended during irrigation practices, except for soils with extremely low permeability	No toxicity risk for most plants
70–85	Low restriction (LR)	Recommended for irrigated soils with light texture or moderate permeability, with salt leaching advised. Sodicity risk may occur in heavy-textured soils, so use should be avoided in soils with high clay content (2:1 clay types)	Avoid salt-sensitive plants
55–70	Moderate restriction (MR)	Suitable for soils with moderate to high permeability. Moderate leaching of salts is suggested	Plants with moderate salt tolerance can be cultivated
40–55	High restriction (HR)	Applicable for soils with high permeability and no compact layers. Frequent irrigation is required when EC > 2000 dS/m and SAR > 7	Suitable for plants with moderate to high salt tolerance. Special salinity control practices are recommended, except when Na^+, Cl^-, and HCO_3^- values are low
0–40	Severe restriction (SR)	Generally unsuitable for irrigation. May be used occasionally under special conditions. For low-salt, high-SAR water, gypsum application is necessary. For highly saline water, soils should be highly permeable, and excess water must be applied to prevent salt accumulation	Only highly salt-tolerant plants should be irrigated, except with waters that have extremely low Na^+, Cl^-, and HCO_3^- levels

PTE Load

The evaluation of groundwater quality for PTE load was performed using the following geo-environmental indices: C_d, HPI, and HEI. Detail description and information for each index is provided below:

Contamination index (C_d): The C_d indicates the extent of contamination or the cumulative effect of various water quality parameters that are considered harmful for domestic use [79]; C_d represents the sum of all contamination factors that exceed permissible limits, calculated using Equation (26).

$$C_d = \sum_{i=1}^{n} C_{fi} \tag{26}$$

where $C_{fi} = \frac{C_{Ai}}{C_{Ni}} - 1$ rerepresents the contamination factor. Herein, C_{Ai} refers to the measured value and C_{Ni} is the upper permissible concentration of the ith parameter. The letter 'N' stands for 'normative value', with C_{Ni} being equivalent to the maximum allowable concentration (MAC). C_d values are typically classified into three categories based on contamination levels: low ($C_d < 1$), medium ($C_d = 1$–3), and high ($C_d > 3$).

Heavy metal pollution index (HPI): The HPI is an effective tool for assessing groundwater pollution, reflecting the combined impact of various PTEs on overall water quality. This methodology, originally developed by Horton [53], assigns weights to each PTE in groundwater samples based on their potential hazards to human health. To calculate HPI, a weight (W_i) is assigned to each variable, with pollutant criteria selected accordingly. The rat-

ing ranges from 0 to 1, indicating the relative significance assigned to specific water quality parameters. This rating is determined using an inverse proportionality function, based on the recommended standard (S_i) for each component. The concentration thresholds—where 'S_i' represents the standard value and 'I_i' the ideal value—are based on guidelines set by the WHO [76]. HPI is calculated using Equations (27) and (28):

$$HPI = \frac{\sum_{i=1}^{n} W_i Q_i}{\sum_{i=1}^{n} W_i} \tag{27}$$

where Q_i represents the sub-index of the ith parameter, W_i is the unit weight assigned to the ith parameter, and *n* is the total number of parameters considered. The sub-index Q_i is calculated as follows (Equation (28)):

$$Q_i = \sum_{i=1}^{n} \frac{|M_i - I_i|}{S_i - I_i} \tag{28}$$

where M_i is the monitored value of the PTE for the ith parameter, I_i is the ideal value (the maximum desirable level for drinking water), and S_i is the standard value (the highest permissible level for drinking water) of the ith parameter. The minus sign (-) in the equation indicates the numerical difference between the two values, disregarding the algebraic sign. Water quality is classified into two categories based on HPI: suitable (HPI < 100) and unsuitable (HPI > 100). The concentration limits, including the highest permissible value (S_i) and the maximum desirable value (I_i) for each parameter, were sourced from the WHO [76].

Heavy metal evaluation index (HEI): HEI is used to assess the overall water quality based on the concentrations of PTEs. Like HPI, it provides insight into water's quality concerning PTE contamination [80]. HEI is calculated using Equation (29):

$$HEI = \sum_{i=1}^{n} \frac{Hc_i}{Hmac_i} \tag{29}$$

where Hc_i represents the measured value of the ith parameter, and H_{maci} refers to the MAC of that parameter. This index is valuable for assessing pollution levels, and its straightforward calculation makes it particularly useful [80,81]. HEI values typically categorize contamination into three levels based on contamination: low (HEI < 10), medium (HEI = 10–20), and high (HEI > 20).

Ionic Ratios

Groundwater quality was evaluated using various ionic ratios, including Ca/Mg, Ca/SO₄, Ca/Na, Cl/NO₃, Cl/HCO₃, and Si/NO₃. Each ionic ratio offers insights into underlying hydrogeochemistry, such as the origin of water from specific geological formations, various geochemical processes, anthropogenic influences, etc.

2.3.2. Statistics

The statistical analysis included descriptive, correlation, and multivariate techniques. Descriptive statistics, such as the mean, minimum, maximum, median, standard deviation, and first and third quartiles, were calculated. For chemical parameters below the detection limit (BDL), values were substituted with the detection limit (DL) to enable further analysis. Spearman's non-parametric rank correlation coefficient (r) [82] was used to assess the association between geo-environmental indices. Correlation coefficients, ranging from -1 to 1, were categorized as very strong (0.8–1), strong (0.6–0.79), moderate (0.4–0.59), weak (0.2–0.39), and very weak (0–0.2) [83]. Two multivariate statistical methods—factor analysis
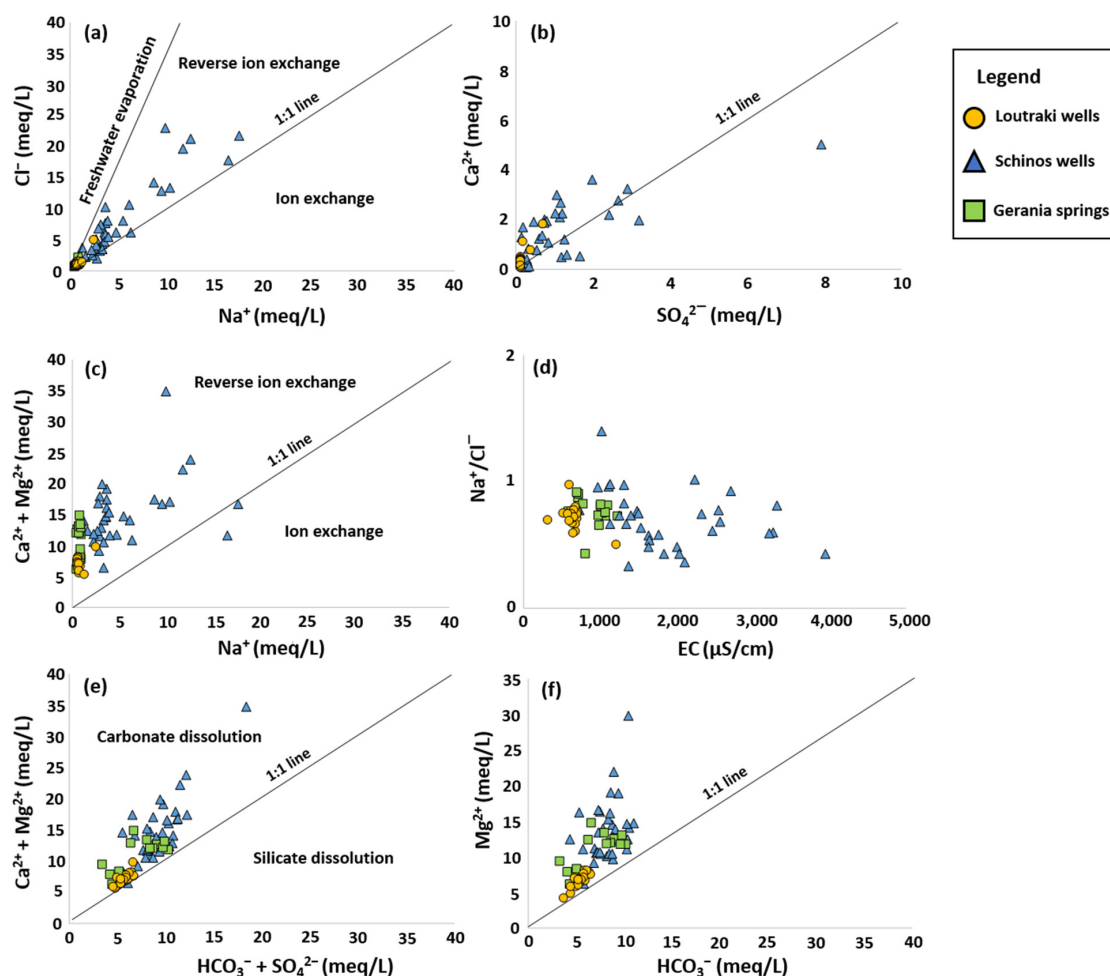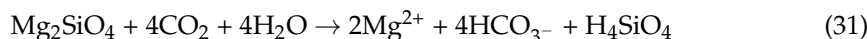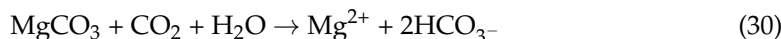
(FA) and hierarchical cluster analysis (HCA)—were employed. Generally, multivariate statistical methods are commonly applied to independent variables, but they can also be used with dependent variables, depending on the objectives of the analysis [83–85]. To meet the normality assumption, the input data were transformed into normal scores. The FA technique was employed to examine interrelationships among parameters, reduce dimensionality, and identify underlying factors. Principal component analysis (PCA) with Varimax rotation [86] was conducted, retaining only factors with eigenvalues greater than or equal to 1, in accordance with Kaiser's criterion [87]. Factor loadings were classified as strong (0.75–1), moderate (0.5–0.75), or weak (0.3–0.5) [88,89]. The Kaiser–Meyer–Olkin (KMO) test [90] and Bartlett's test [91] were used to assess data adequacy. An HCA approach, using Ward's method [92] and squared Euclidean distances, was performed in R-mode to classify geo-environmental indices based on similarity. All statistical analyses were conducted using IBM SPSS v.22 (IBM Corp., Armonk, NY, USA).

3. Results and Discussion

3.1. Hydrogeochemical Characteristics

The groundwater samples from the study area exhibit alkaline (pH $\geq$ 7.45; from 7.45 to 9.64) and oxidizing (Eh $\geq$ 231 mV; from 231 mV to 371 mV) geochemical conditions [30]. The EC values range from 316 μS/cm to 3943 μS/cm, while DO values vary from 3.62 mg/L to 13.49 mg/L [30], suggesting the influence of diverse hydrogeochemical processes on groundwater quality. Previous studies have identified factors/processes such as seawater intrusion [28–30] and initial stages of denitrification [30] as potential contributors to these variations. More information about the descriptive statistics of the above-mentioned dataset is presented in the study by Papazotos et al. [30]. The Schinos area consistently showed the lowest pH values, while the highest were observed in the springs of the Gerania Mts. The groundwater was predominantly classified as Mg-HCO^3 water type, which indicates rainwater–ultramafic rock/soil interaction, as confirmed by the Piper plot presented in our previous work [30]. In the Loutraki area and Gerania Mts., Mg^{2+} concentrations among major cations exceeded those of Ca^{2+} or alkali (Na$^+$ + K$^+$), whereas Schinos displayed both high Mg^{2+} and alkali levels. Regarding major anions, HCO$_{3-}$ predominated in the region, followed by Cl$^-$, with the samples of the Schinos area showing elevated Cl$^-$ concentrations. The main hydrochemical types were Mg-HCO$_3$, Mg-Cl, and Na-Cl, with samples of the Schinos area suggesting possible seawater intrusion due to increased Na$^+$ and Cl$^-$; these results are in agreement with previous studies in the same area (e.g., [28–30,33]). Bivariate diagrams were employed to further explore these hydrogeochemical relationships (Figure 3). The strong linear correlations observed between Na$^+$ vs. Cl$^-$, as well as Ca^{2+} vs. SO$_4^{2-}$, indicate a shared origin for these ions, evidenced by their alignment along the theoretical 1:1 line associated with halite and gypsum dissolution (Figure 3a,b). The samples from the Schinos area exhibited notably higher groundwater concentrations of dissolved ions. This alignment strongly suggests that seawater intrusion plays a major role as a driving geochemical process in the study area. Additionally, the majority of the samples exhibited a minor deviation, plotting above the 1:1 line in the Ca + Mg vs. Na plot (Figure 3c). This pattern underscores the importance of reverse cation exchange as a significant geochemical process, marked by a decrease in Na$^+$ and an increase in other major cations, particularly Ca^{2+} and Mg^{2+} [89,93]. In Figure 3d, a slight decrease in the Na$^+$/Cl$^-$ ratio is observed as EC increases, further supporting the presence of a seawater intrusion regime in the Schinos area, where EC values reached up to 3943 μS/cm [30]. The presence of Mg^{2+} in groundwater is primarily associated with the abundance of Mg-bearing silicate minerals found in ultramafic rocks in the study area [30,31], such as those in the olivine (e.g., forsterite [Mg$_2$SiO$_4$]), and pyroxene (e.g., enstatite [Mg$_2$Si$_2$O$_6$]) groups, as well as secondary minerals

such as the serpentine group $[Mg_3Si_2O_5(OH)_4]$ and talc $[Mg_3Si_4O_{10}(OH)_2]$. Additionally, significant contributions of Mg^{2+} result from the dissolution Mg-rich carbonates, including magnesite $[MgCO_3]$, hydromagnesite $[Mg_5(CO_3)_4(OH)_2 \cdot 4(H_2O)]$, huntite $[Mg_3Ca(CO_3)_4]$, and pyroaurite $[Mg_6Fe^{3+}_2CO_3(OH)_{16} \cdot 4H_2O]$ [94], a process that may explain the observed predominance of $HCO_{3-} + SO_4^{2-}$ over $Ca^{2+} + Mg^{2+}$ (Figure 3e). This process can be represented by the following dissolution reactions for magnesite (Equation (30)) and forsterite (Equation (31)), which also apply to other relevant mineral phases:

$$MgCO_3 + CO_2 + H_2O \rightarrow Mg^{2+} + 2HCO_{3-} \tag{30}$$

$$Mg_2SiO_4 + 4CO_2 + 4H_2O \rightarrow 2Mg^{2+} + 4HCO_{3-} + H_4SiO_4 \tag{31}$$

Figure 3. Cross-plots of (**a**) Na^+ vs. Cl^-, (**b**) SO_4^{2-} vs. Ca^{2+}, (**c**) Na^+ vs. $(Ca^{2+} + Mg^{2+})$, (**d**) EC vs. Na^+/Cl^-, (**e**) $(HCO_{3-} + SO_4^{2-})$ vs. $(Ca^{2+} + Mg^{2+})$, and (**f**) HCO_{3-} vs. Mg^{2+} for the 68 groundwater samples from the Loutraki–Schinos–Gerania Mts. region.

However, the higher concentrations of Mg^{2+} compared to HCO_{3-} (Figure 3f), particularly evident in the Schinos area, suggest an additional source of Mg^{2+} in the groundwater, likely due to seawater intrusion and reverse ion exchange processes.

The Ficklin diagram (Figure 4) demonstrates that although concentrations of PTEs tend to increase with decreasing pH, the overall levels of PTEs in the groundwater remain relatively low based on the diagram's classification [95]. Typically, most PTEs in groundwater exist as cations, and their mobilization requires acidic conditions. As a result, the alkaline conditions prevalent throughout the region generally inhibit their mobility.

However, elevated groundwater concentrations of specific PTEs, such as Cr, Cr(VI), and As, were detected, particularly in the Schinos area [30]. These PTEs form oxyanions, which have a different geochemical mobility compared to cations, allowing them to remain mobile even under alkaline pH conditions.
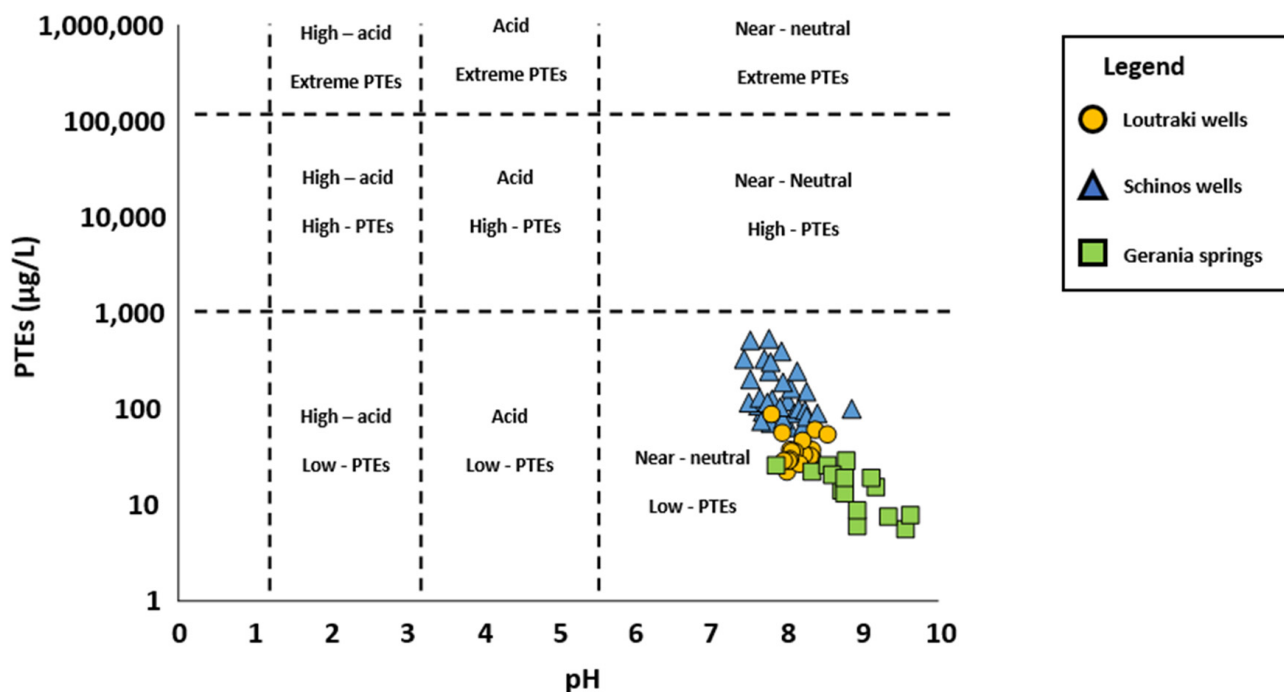

Figure 4. Ficklin diagram [95] of 68 groundwater samples showing the sum of PTEs vs. pH.

It is important to note that the Schinos area dominates a seawater intrusion regime, leading to the salinization of groundwater. This phenomenon is evidenced by elevated groundwater concentrations of Cl^- and Na^+, which are typically abundant in seawater [30]. In contrast, the Gerania Mts. and the Loutraki area are dominated by ultramafic rocks composed of Mg-rich minerals, resulting in high groundwater concentrations of Mg^{2+}, while Ca^{2+} concentrations remain notably low in the same regions.

The absence of significant anthropogenic activities in the study area is confirmed by the low NO_3^- groundwater concentrations. However, in the Schinos area, concentrations exceeding 50 mg/L are observed, surpassing the guideline values set by the WHO [76] and Greek legislation (FEK B 3525/25.05.2023). This increase is likely attributable to relatively limited anthropogenic influences on the environment (e.g., small-scale farming, irrigation, low-impact tourism), with fertilizers and septic tanks identified as potential sources of contamination [28,30,33].

Notably, groundwater in the Schinos area exhibits significantly higher concentrations of Cr and Cr(VI), along with notable levels of As. Previous studies link elevated Cr and Cr(VI) levels to synergistic anthropogenic effects, such as fertilizer use and septic tanks, particularly in Cr-rich environments influenced by ultramafic rocks and soils [30,33,89]. In contrast, the occurrence and mobilization of As in groundwater is associated with the prevailing seawater intrusion regime and specific geochemical processes that are related to N-cycling. The combination of seawater intrusion and denitrification processes creates favorable conditions for the mobilization and release of As into the groundwater [30].

3.2. Groundwater Quality Evaluation for Various Purposes

The geo-environmental indices calculated and assessed for groundwater suitability and quality in the study area are categorized into the following four groups, as outlined in Sections 3.2.1–3.2.4:

- Drinking water quality indices
- Irrigation water quality indices
- PTE load indices
- Ionic ratios

Overall, the geo-environmental indices discussed have been widely used to assess groundwater suitability and quality across all continents and countries worldwide, such as Nigeria [22,96], Iran [97], Algeria [98], Morocco [99,100], Ethiopia [101], Brazil [74], Poland [102], Syria [103], China [104], United Arab Emirates [105], Turkey [106], India [107,108], Australia [109], Spain, [110], etc. These indices have proven invaluable in identifying areas where groundwater quality is compromised, revealing patterns and factors that influence water usability for drinking, irrigation, and other purposes. Studies consistently report that poor water quality globally is shaped by a combination of anthropogenic and geogenic factors. Among these, nitrate pollution emerges as a significant contributor. Elevated groundwater concentrations of NO_3^- often result from agricultural activities, particularly the use of chemical fertilizers, as well as from improper waste disposal, and sewage infiltration. These processes introduce excessive NO_3^- into groundwater systems, leading to a decline in overall water quality and suitability for human consumption and agricultural use [99,103,108,111–113]. Another critical factor affecting groundwater quality is salinization. This phenomenon is characterized by high levels of Cl^- in groundwater, which can be attributed to several causes, such as seawater intrusion into coastal aquifers, the presence of ancient saline formations, the weathering of salt-rich rocks, and the dissolution of halide minerals. Such conditions not only compromise the usability of groundwater for drinking but also pose challenges for agricultural irrigation and soil health [99,103,113,114]. In addition to these processes, additional human activities have been shown to exacerbate groundwater contamination. Industrial operations, mining activities, and changes in land use often introduce pollutants into aquifers, further reducing water quality. The discharge of industrial effluents and the alteration of natural landscapes can mobilize harmful substances into groundwater systems, making them less suitable for any form of use [23,115–118]. Lastly, geogenic factors play a significant role in shaping groundwater quality. Naturally occurring processes such as the dissolution of host rock minerals release PTEs and major dissolved ions into aquifers. While these processes are natural, their contributions to groundwater chemistry can significantly influence the values of geo-environmental indices, particularly in areas with specific geological conditions [113,119,120]. All the factors mentioned above directly influence the final scores of geo-environmental indices. These scores not only pinpoint areas requiring close monitoring but also emphasize the urgent need for effective management strategies to mitigate contamination from both anthropogenic and geogenic sources.

3.2.1. Drinking Purposes

To assess groundwater suitability for drinking purposes, five geo-environmental indices—NPI, RI, PIG, WQI, and WPI—were calculated, with the results summarized in Table 4. The majority of the samples suggest that groundwater quality is generally good and meets the standards for drinking, based on the indices analyzed. However, specific samples, particularly those evaluated by the NPI and PIG indices, are classified as unsuitable for drinking. These samples, predominantly from the Schinos area, display elevated concentrations of certain major elements (e.g., Cl^-, Na^+, NO_3^-). Additionally,

it is important to emphasize that these geo-environmental indices neglect the influence of determined PTEs, whose toxicity can pose serious risks to human health and other living organisms.

Table 4. The number and percentage of samples for five geo-environmental indices (NPI, RI, PIG, WQI, and WPI), and related to drinking purposes, based on 20 groundwater samples from the Loutraki area, 33 samples from the Schinos area, and 15 samples from the Gerania Mts.

Geo-Environmental Index	Classes	Description	Total		Loutraki Area		Schinos Area		Gerania Mts.	
			N	%	N	%	N	%	N	%
NPI	<0	Clean	33	48.5	17	85	3	9.1	13	86.7
	0–1	Lightly polluted	12	17.6	3	15	7	21.2	2	13.3
	1–2	Moderately polluted	5	7.4	0	0	5	15.2	0	0
	2–3	Significantly polluted	4	5.9	0	0	4	12.1	0	0
	>3	Very significantly polluted	14	20.6	0	0	14	42.4	0	0
RI	<0.5	Unaffected	44	64.7	19	95	11	33.3	14	93.3
	0.5–6.6	Slightly affected	24	35.3	1	5	22	66.7	1	6.7
	>6.6	Strongly affected	0	0	0	0	0	0	0	0
PIG	<1	No significant pollution	39	57.4	20	100	4	12.1	15	100
	1–1.5	Low pollution	17	25.0	0	0	17	51.5	0	0
	1.5–2	Moderate pollution	8	11.8	0	0	8	24.2	0	0
	2–2.5	High pollution	3	4.4	0	0	3	9.1	0	0
	>2.5	Very high pollution	1	1.5	0	0	1	3.0	0	0
WQI	<50	Excellent	46	67.6	20	100	11	33.3	15	100
	50–100	Good	19	27.9	0	0	19	57.6	0	0
	100–200	Poor	3	4.4	0	0	3	9.1	0	0
	200–300	Very poor	0	0.0	0	0	0	0.0	0	0
	>300	Unsuitable	0	0.0	0	0	0	0.0	0	0
WPI	<0.5	Excellent	52	76.5	20	100	16	48.5	15	100
	0.5–0.75	Good	14	20.6	0	0	14	42.4	0	0
	0.75–1	Moderately polluted	3	4.4	0	0	3	9.1	0	0
	>1	Highly polluted	0	0	0	0	0	0	0	0

3.2.2. Irrigation Purposes

To evaluate groundwater suitability for irrigation, indices such as SAR, KR, %Na, PS, MAR, RSC, SSP, TH, PI, IWQI, and TDS were calculated, analyzed, and assessed. According to established classification systems, most indices suggest that groundwater in the study areas is suitable for irrigation, posing minimal health risks and having only minor impacts on soil quality (Table 5). However, some indices, particularly the PS index in certain Schinos samples, indicate moderate water quality. This index, which incorporates Cl^-, showed elevated values in areas experiencing groundwater salinization, such as the Schinos coastal aquifer [28,30]. These findings illustrate that different geo-environmental indices applied to the same water samples within the same area can yield contrasting results, due to variations in the parameters each index evaluates, whether cations, anions, or other chemical elements.

Table 5. The number and percentage of samples for 11 geo-environmental indices (SAR, KR, %Na, PS, MAR, RSC, SSP, TH, PI, IWQI, and TDS), and related to irrigation purposes, based on 20 groundwater samples from the Loutraki area, 33 samples from the Schinos area, and 15 samples from the Gerania Mts.

Geo-Environmental Index	Classes	Description	Total		Loutraki Area		Schinos Area		Gerania Mts.	
			N	%	N	%	N	%	N	%
SAR	<10	Excellent	68	100	20	100	33	100	15	100
	10–18	Good	0	0	0	0	0	0	0	0
	18–26	Doubtful	0	0	0	0	0	0	0	0
	>26	Unsuitable	0	0	0	0	0	0	0	0
KR	<1	Suitable	66	97.1	20	100	31	93.9	15	100
	>1	Unsuitable	2	2.94	0	0	2	6.06	0	0
%Na	<20%	Excellent	50	73.5	20	100	15	45.5	15	100
	20–40%	Good	16	23.5	0	0	16	48.5	0	0
	40–60%	Permissible	2	2.94	0	0	2	6.06	0	0
	60–80%	Doubtful	0	0	0	0	0	0	0	0
	>80%	Unsuitable	0	0	0	0	0	0	0	0
PS	<3	Safe	37	54.4	19	95	3	9.09	15	100
	>3	Unsafe	31	45.6	1	5	30	90.9	0	0
MAR	<50	Suitable	0	0	0	0	0	0	0	0
	>50	Unsuitable	68	100	20	100	33	100	15	100
RSC	<1.25	Good	68	100	20	100	33	100	15	100
	1.25–2.5	Moderate	0	0	0	0	0	0	0	0
	>2.5	Unsuitable	0	0	0	0	0	0	0	0
SSP	<50	Suitable	66	97.1	20	100	31	93.9	15	100
	>50	Unsuitable	2	2.94	0	0	2	6.06	0	0
TH	<60 mg/L	Soft	0	0	0	0	0	0	0	0
	60–120 mg/L	Moderately hard	0	0	0	0	0	0	0	0
	120–180 mg/L	Hard	0	0	0	0	0	0	0	0
	>180 mg/L	Very hard	68	100	20	100	33	100	15	100
PI	>75%	Suitable	0	0	0	0	0	0	0	0
	25–75%	Good	67	98.5	20	100	33	100	14	93.3
	<25%	Unsuitable	1	1.47	0	0	0	0	1	6.67
IWQI	85–100	No restriction	0	0	0	0	0	0	0	0
	70–85	Low restriction	15	22.1	6	30	4	12.1	5	33.3
	55–70	Moderate Restriction	39	57.4	14	70	19	57.6	6	40
	40–55	High restriction	8	11.8	0	0	4	12.1	4	26.7
	0–40	Severe restriction	6	8.82	0	0	6	18.2	0	0
TDS	>500 mg/L	Unsuitable	48	70.6	6	30	33	100	9	60
	<500 mg/L	Suitable	20	29.4	14	70	0	0	6	40

3.2.3. PTE Load Evaluation

The geo-environmental indices applied to assess PTEs in this study include Cd, HPI, and HEI. These indices provide a basis for evaluating water quality concerning trace elements for determining water usability. Elements included in these calculations—such as As, Cr, Cu, Mn, Ni, Pb, Sb, Co, and Zn—represent key PTEs with environmental significance, as highlighted in recent studies [121]. Results indicate that most samples were classified as suitable for use or of good quality/low contamination (Table 6). However, some groundwater samples from the Schinos area displayed moderate to poor quality due to elevated concentrations of specific PTEs, including Cr [as Cr(VI)] and As [28,30,38].

Table 6. The number and percentage of samples for three geo-environmental indices (C_d, HPI, and HEI), and related to PTE load, based on 20 groundwater samples from the Loutraki area, 33 samples from the Schinos area, and 15 samples from the Gerania Mts.

Geo-Environmental Index	Classes	Description	Total		Loutraki Area		Schinos Area		Gerania Mts.	
			N	%	N	%	N	%	N	%
C_d	<1	Low	68	100	20	100	33	100	15	100
	1–3	Medium	0	0	0	0	0	0	0	0
	>3	High	0	0	0	0	0	0	0	0
HPI	<100	Suitable	53	77.9	19	95	19	57.6	15	100
	>100	Unsuitable	15	22.1	1	5	13	39.4	0	0
HEI	<10	Low	66	97.1	20	100	31	93.9	15	100
	10–20	Medium	2	2.94	0	0	2	6.06	0	0
	>20	High	0	0	0	0	0	0	0	0

3.2.4. Ionic Ratios Results

Ionic ratios offer valuable insights into the hydrogeochemical characteristics of groundwater resources, shedding light on factors such as aquifer matrix lithology, salinization processes, and the differentiation between anthropogenic and geogenic influences. The statistical distributions of the calculated ionic ratios (e.g., Ca/Mg, Ca/SO$_4$, Ca/Na, Cl/NO$_3$, Cl/HCO$_3$, and Si/NO$_3$) are illustrated as boxplots in Figure 5. Notably, groundwater samples from the Schinos area exhibit a broader range in certain ionic ratios, such as Ca/Mg (Figure 5a), Ca/SO$_4$ (Figure 5b), Ca/Na (Figure 5c), Cl/NO$_3$ (Figure 5d), and Cl/HCO$_3$ (Figure 5e), which can be attributed to the intense seawater intrusion regime of this aquifer [28–30], characterized by elevated groundwater concentrations of dissolved ions such as Na$^+$ and Cl$^-$. For Ca/Mg ratios (Figure 5a), the low values recorded in the Loutraki area and the Gerania Mts. suggest the predominance of Mg^{2+} over Ca^{2+}, as previously discussed. For Si/NO$_3$ ratios (Figure 5f), the lower Si/NO$_3$ values in the groundwater of the Schinos area indicate elevated groundwater NO$_{3-}$ concentrations, reflecting the influence of specific anthropogenic activities on groundwater quality. In contrast, samples from the Gerania Mts. display a wide range of Si/NO$_3$ ratios. However, the lower values in this region cannot be attributed to anthropogenic activities, as evidenced by the low NO$_{3-}$ concentrations (up to 15.6 mg/L) and the lack of significant human impact on this sub-basin. Instead, the low Si/NO$_3$ ratios are associated with low Si concentrations (median concentration: 2.76 mg/L; minimum concentration <40 µg/L [30]) in the groundwater, which can be explained by the short groundwater residence time within the aquifer, the limited presence of silicate mineral phases, and their inherently low solubility as previously discussed. These findings underscore the importance of combining ionic ratios with elemental concentration data for a comprehensive understanding of groundwater hydrogeochemistry.

3.3. Coupling Geo-Environmental Indices for Assess the Hydrogeochemical Properties of an Area

The geo-environmental indices examined, though relatively easy to apply, are somewhat limited in scope, as they primarily focus on the concentrations of selected elements, neglecting other PTEs crucial to the health of living organisms and ecosystems. Correlation and multivariate statistical analyses, including FA and R-mode HCA, revealed notable patterns between various geo-environmental indices. Figure 6 presents the Spearman correlation coefficients for 25 calculated parameters based on 68 groundwater samples in the study area. The strongest statistically significant correlations are highlighted using a color-coded scale: positive correlations are depicted in shades ranging from orange to red, while negative correlations are represented by light to dark blue (see Figure 6). Correlations selected for further analysis are those with *p*-values below 0.01 or 0.05.
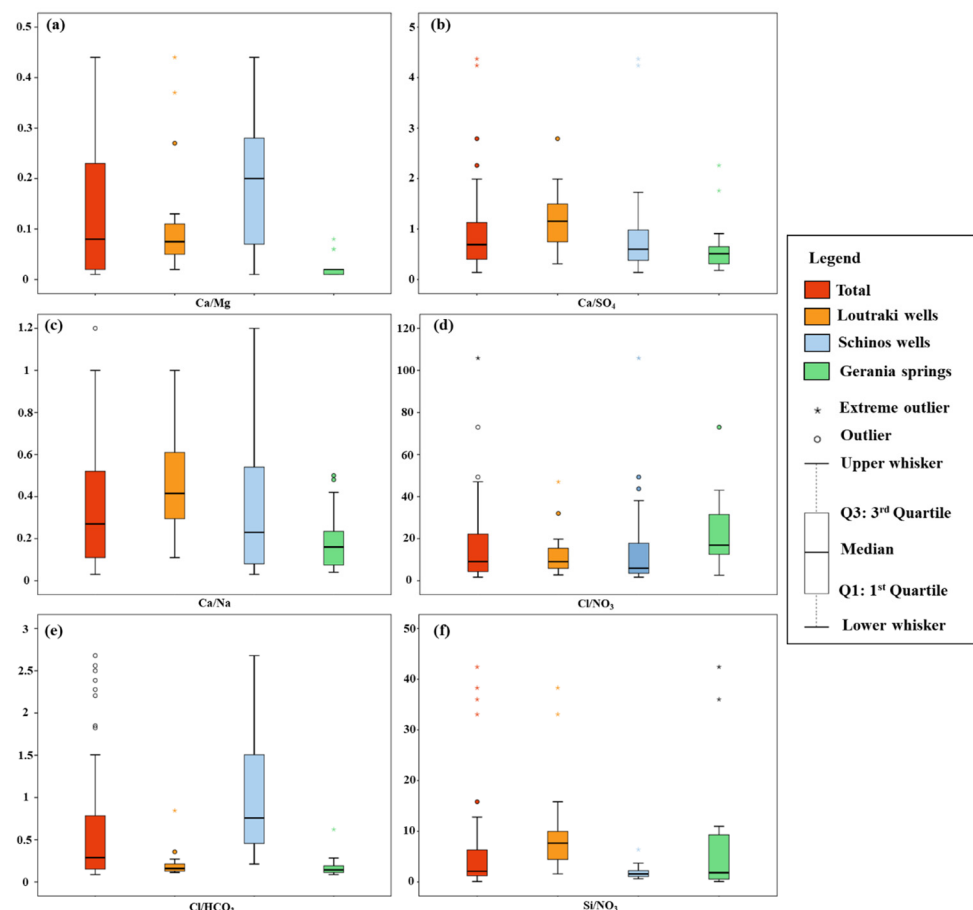
Figure 5. Boxplots of ionic ratios (**a**) Ca/Mg, (**b**) Ca/SO$_4$, (**c**) Ca/Na, (**d**) Cl/NO$_3$, (**e**) Cl/HCO$_3$, and (**f**) Si/NO$_3$ for the groundwater samples from the Loutraki–Schinos–Gerania Mts. region.

It is common for many geo-environmental indices, particularly those related to water quality for drinking purposes, to exhibit very strong, statistically significant correlations such as PIG and WQI (r = 0.977). However, it is especially challenging to explore the statistical patterns among indices associated with different suitability uses or ionic ratios. This evaluation can be effectively carried out using multivariate statistical tools such as FA via the method of PCA and R-mode HCA.

All 25 variables (NPI, RI, PIG, WQI, WPI, SAR, KR, %Na, PS, MAR, RSC, SSP, TH, PI, IWQI, TDS, C$_d$, HPI, HEI, Ca/Mg, Ca/SO$_4$, Ca/Na, Cl/NO$_3$, Cl/HCO$_3$, and Si/NO$_3$) were used to calculate multivariate statistics for the 68 groundwater samples. Geo-environmental indices, calculated using formulas that incorporate determined chemical element data, are inherently dependent variables; however, the literature often treats them as independent variables (e.g., [122,123]). This direction does not constrain our research, as such data are well suited for multivariate statistical analyses [83–85]. Furthermore, the objective of this study is to explore the interrelationships among geo-environmental indices and uncover underlying patterns by grouping these indices to reveal hidden connections. This approach facilitates the identification of key chemical parameters and processes associated with each factor or cluster, enhancing their applicability in environmental science and groundwater pollution studies.

Regarding FA, the scree plot method (Cattell, 1966), depicted in Figure 7, highlights that five components have eigenvalues exceeding 1, meeting Kaiser's criterion [86] for classification as principal components, while the remaining factors are excluded.
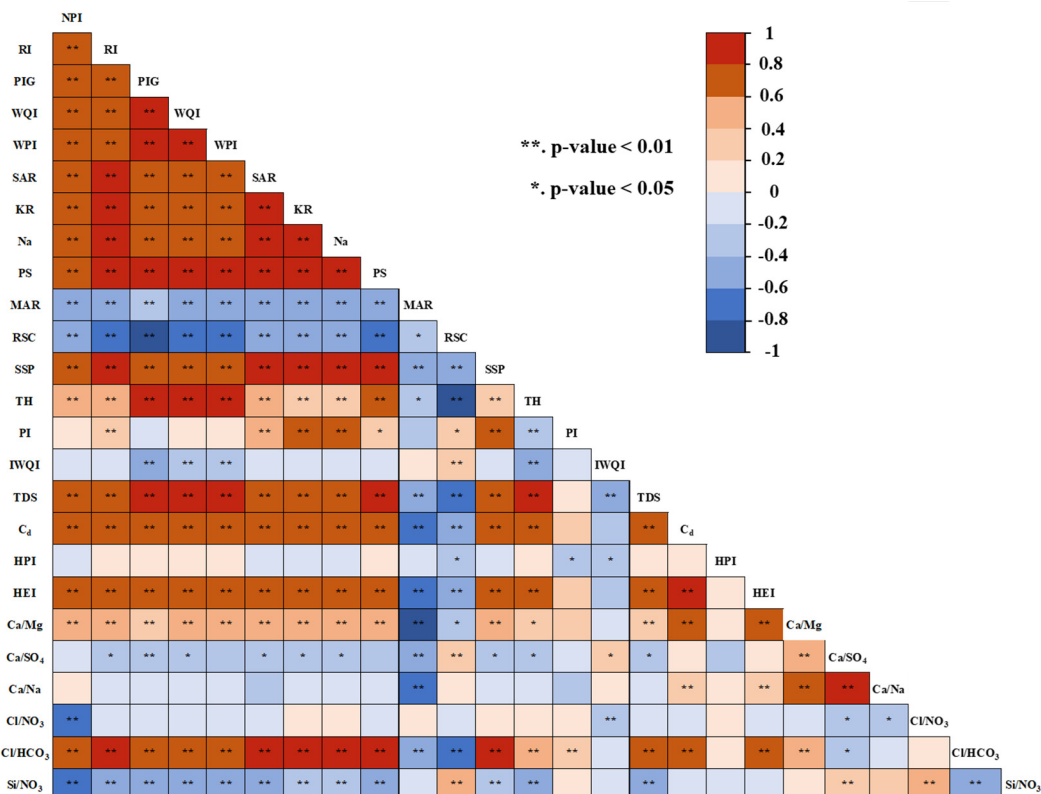
Figure 6. The Spearman correlation matrix, along with significance levels (*p*-values), for the 25 calculated geo-environmental indices in the Loutraki–Schinos–Gerania Mts. region (n = 68 groundwater samples).
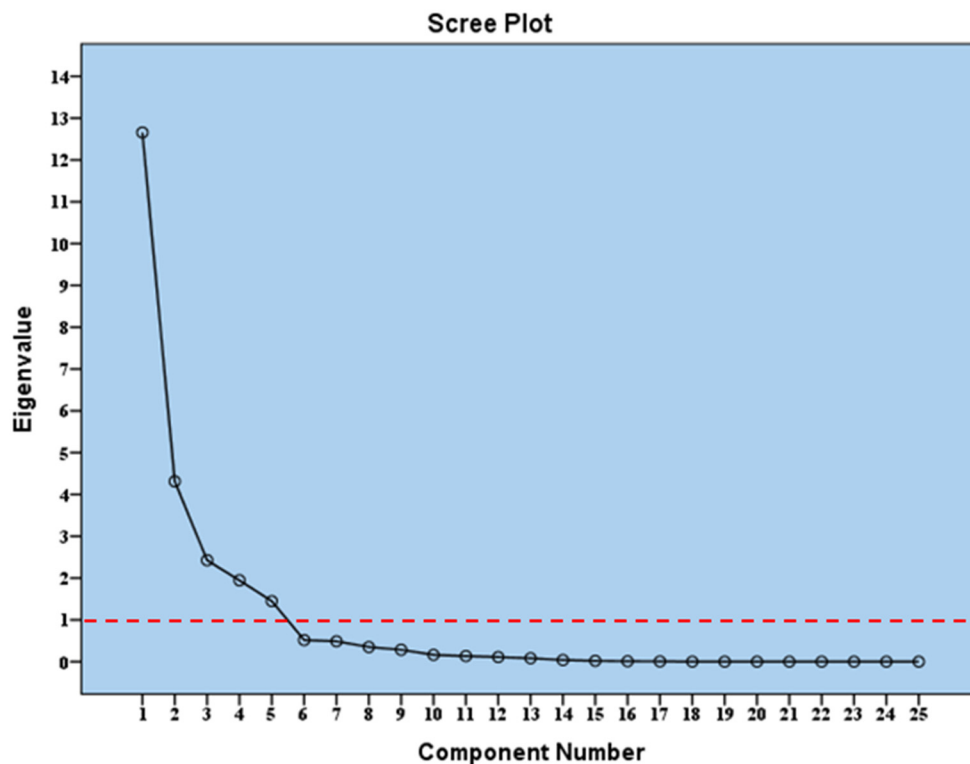
Figure 7. The scree plot of eigenvalues for the components derived from 68 groundwater samples collected from the Loutraki–Schinos–Gerania Mts. region indicates that five components have eigenvalues > 1, signifying their statistical significance within the FA approach.

The five factors explained 91.162% of the total data variance. The KMO value is equal to 0.673, indicating statistically significant results. Additionally, Bartlett's test of sphericity yielded a *p*-value < 0.05, confirming the validity and suitability of the data for FA. These two criteria, KMO and Bartlett's test of sphericity, are widely used in geochemical studies (e.g., [17,21,89]) and are necessary to verify the quality of the multivariate statistical analysis. Table 7 presents the outcomes of the FA, conducted using the PCA method, for the 68 groundwater samples from the Loutraki–Schinos–Gerania Mts. region. The parameter loadings are color-coded: strong loadings are shown in red, moderate loadings in light orange, and weak loadings in light blue. The results of the FA are presented in Table 7 and can be summarized as follows:

- The first factor (FA1) accounts for 50.629% of the total variance. It features strong positive loadings for variables TH (0.97), PIG (0.94), TDS (0.90), WQI (0.87), WPI (0.86), and PS (0.84). Additionally, it includes a strong negative loading for RSC (−0.92); moderate positive loadings for RI (0.71), Cl/HCO$_3$ (0.71), and SAR (0.52); a moderate negative loading for IWQI (−0.68); and weak positive loadings for KR (0.36), SSP (0.41), %Na (0.41), C$_d$ (0.31), HEI (0.31), Cl/NO$_3$ (0.46), and NPI (0.37).
- The second factor (FA2) explains 17.251% of the total variance. It shows strong positive loadings for PI (0.95), KR (0.91), SSP (0.89), %Na (0.89), and SAR (0.83). Moderate positive loadings are observed for PS (0.50), RI (0.61), and Cl/HCO$_3$ (0.61), while weak positive loadings appear for TDS (0.36), WQI (0.37), and WPI (0.36). There is also a weak negative loading for IWQI (−0.39).
- The third factor (FA3) accounts for 9.708% of the total variance, with strong positive loadings for HPI (0.94), C$_d$ (0.87), and HEI (0.87); a weak positive loading for Ca/Mg (0.39); and a weak negative loading for MAR (−0.39).
- The fourth factor (FA4) explains 7.781% of the total variance. It includes strong positive loadings for Ca/Na (0.87), Ca/SO$_4$ (0.80), and Ca/Mg (0.79); a strong negative loading for MAR (−0.80); and weak positive loadings for NPI (0.34) and Si/NO$_3$ (0.38).
- The fifth factor (FA5) accounts for 5.793% of the total variance and features a strong negative loading for Cl/NO$_3$ (−0.79), a moderate positive loading for NPI (0.74), and a moderate negative loading for Si/NO$_3$ (−0.69).

Table 7. Varimax-rotated principal components of 68 groundwater samples from the Loutraki–Schinos–Gerania Mts. region; strong, moderate, and weak loadings of the parameters are given with red, orange, and blue colors, respectively.

Geo-Environmental Index	Component				
	FA1	FA2	FA3	FA4	FA5
TH	**0.97**	−0.03	0.19	0.03	0.07
PIG	**0.94**	0.25	0.15	0.06	0.14
RSC	**−0.92**	−0.01	−0.29	−0.01	0.08
TDS	**0.90**	0.36	0.10	0.05	0.09
WQI	**0.87**	0.37	0.16	0.12	0.23
WPI	**0.86**	0.36	0.17	0.11	0.24
PS	**0.84**	0.50	0.12	0.01	−0.06
RI	**0.71**	0.61	0.19	−0.01	−0.06
Cl/HCO$_3$	**0.71**	0.61	0.19	−0.01	−0.06
IWQI	**−0.68**	−0.39	0.01	0.16	0.21
PI	−0.15	**0.95**	−0.14	0.00	−0.02
KR	0.36	**0.91**	0.04	−0.07	0.01
SSP	0.41	**0.89**	0.08	−0.02	0.09
%Na	0.41	**0.89**	0.08	−0.02	0.09
SAR	0.52	**0.83**	0.06	−0.07	−0.01
HPI	0.06	−0.06	**0.94**	0.03	−0.02
C$_d$	0.31	0.08	**0.87**	0.23	0.19

Table 7. *Cont.*

Geo-Environmental Index	Component				
	FA1	**FA2**	**FA3**	**FA4**	**FA5**
HEI	0.31	0.08	**0.87**	0.23	0.19
Ca/Na	−0.06	−0.27	0.22	**0.87**	−0.02
Ca/SO$_4$	−0.20	−0.16	−0.23	**0.80**	−0.02
MAR	−0.28	−0.22	−0.39	**−0.80**	−0.08
Ca/Mg	0.27	0.21	0.39	**0.79**	0.06
Cl/NO$_3$	0.46	0.10	−0.04	−0.08	**−0.79**
NPI	0.37	0.07	0.21	0.34	**0.74**
Si/NO$_3$	−0.26	−0.10	−0.12	0.38	**−0.69**
Initial eigenvalues of variances in %	**50.629**	**17.251**	**9.708**	**7.781**	**5.793**
Cumulative % of variance	**50.629**	**67.880**	**77.588**	**85.370**	**91.162**

Bold values indicate significant score loadings.

These five factors collectively explain the majority of the variance in the data, highlighting the most influential variables.

On the other hand, the R-mode HCA employed Ward's method (1963) as the linkage rule, using squared Euclidean distances to measure similarity between variables, a method that is extensively utilized in other geochemical studies (e.g., [101,124,125]). The dendrogram in Figure 8 illustrates the results of the R-mode HCA, depicting 68 groundwater samples collected from the Loutraki–Schinos–Gerania Mts. region. Variables with a linkage distance equal to eight (marked by the red dashed line in Figure 8) and equal to five (indicated by the yellow dashed line in Figure 8) were clustered together, forming distinct groups characterized by similar patterns. As shown in the dendrogram (Figure 8), the variables were partitioned into six clusters at lower linkage distances and three clusters at greater linkage distances. The relationship between the two approaches is that the additional clusters formed by the yellow dashed line represent proximity between specific variables. These variables are grouped together at a higher linkage distance, as indicated by the red dashed line. The three clusters created from a linkage distance equal to eight are as follows:

- Cluster C1: C$_d$, HEI, HPI, NPI, and Ca/Mg.
- Cluster C2: %Na, SSP, SAR, KR, PI, RI, Cl/HCO$_3$, PS, WQI, WPI, TDS, PIG, and TH.
- Cluster C3: RSC, IWQI, MAR, Ca/SO$_4$, Ca/Na, Cl/NO$_3$, and Si/NO$_3$

The six clusters created from a linkage distance equal to five are as follows:

- Cluster C1: C$_d$, HEI, HPI, NPI, and Ca/Mg.
- Cluster C2A: %Na, SSP, SAR, KR, and PI.
- Cluster C2B: RI, Cl/HCO$_3$, PS, WQI, WPI, TDS, PIG, and TH.
- Cluster C3A: RSC, IWQI, and MAR.
- Cluster C3B: Ca/SO$_4$ and Ca/Na.
- Cluster C3C: Cl/NO$_3$ and Si/NO$_3$.

Considering the results of correlation and multivariate statistical analyses, distinct patterns emerge among the geo-environmental indices. FA1 reflects indices that are strongly influenced by elevated concentrations of dissolved major ions, such as TH, PIG, TDS, WQI, WPI, RI, and Cl/HCO$_3$. In particular, the strong negative loadings of RSC and IWQI in this factor indicate the influence of alkalinity on other ions in the aqueous solution. Notably, ions like HCO$_{3-}$ and Cl$^-$, which occur in higher concentrations, play a key role in defining the geo-environmental indices associated with this factor. Processes that increase dissolved salts in groundwater, such as seawater intrusion, exert a significant influence on these geo-environmental indices. This is further confirmed by the Spearman's correlation coefficients and the R-mode HCA (cluster C2B), which highlight the close relationships

among these indices. Additionally, Na-related indices are included in this category due to the strong positive correlation observed between Cl^- and Na^+ in most hydrogeochemical studies (e.g., [89]). FA2 identifies a group of Na-related indices, such as PI, SAR, %Na, KR, and SSP, with their proximity further supported by cluster C2A of the HCA. FA3 points to indices related to the presence of PTEs in groundwater, such as C_d, HEI, and HPI; these indices are grouped within C1 of the HCA. FA4 highlights a group of Ca-related indices, such as Ca/Na, Ca/SO$_4$, Ca/Mg, and MAR. The negative loading of MAR is linked to the inverse relationship of Ca, where high Ca levels correspond with low MAR values. It is important to note that some of the indices mentioned above belong to different HCA clusters, reflecting different interpretations for each group. For instance, the Ca/Mg ionic ratio is part of C1, indicating its relationship with PTE loadings in groundwater or anthropogenic influences, due to the presence of PTE-related indices and NPI. In contrast, MAR, Ca/SO$_4$, and Ca/Na are grouped in C3, indicating that this cluster is associated with increased dissolved salts in groundwater. Lastly, FA5 highlights indices such as NPI, Si/NO$_3$, and Cl/NO$_3$, which reveal anthropogenic influences in the area. These indices also provide insights into other hydrogeochemical processes, including geogenic contributions, seawater intrusion, and the specific sources of N in the environment.
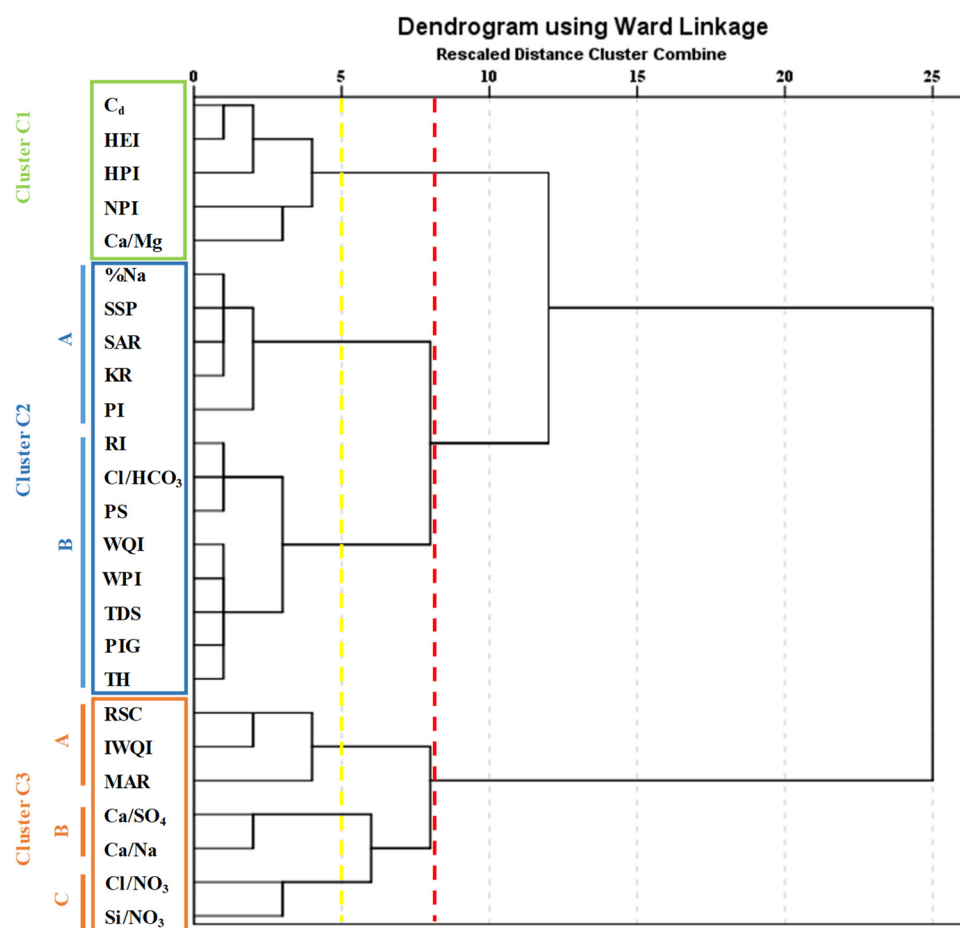

Figure 8. Dendrogram of R-mode HCA for 25 variables calculated in 68 groundwater samples from the Loutraki–Schinos–Gerania Mts. region. The red and yellow dashed lines represent the linkage distances used to create different distinct clusters.

The results of the geo-environmental indices and their statistical analysis indicate that many indices exhibit significant similarities, making it unnecessary to calculate all of them. Specifically, the identified strong, statistically significant correlations suggest that

successful groundwater suitability assessments and hydrogeochemical evaluations can be achieved without relying on an extensive number of geo-environmental indices. However, the selection of appropriate geo-environmental indices remains challenging, as it depends on various factors, including geology, land use, anthropogenic activities, proximity to the sea, etc. Therefore, we strongly recommend prioritizing the efficient utilization of selected indices and adopting a more robust methodological framework, both of which are crucial in the scientific disciplines of hydrogeochemistry and groundwater management. Focusing on key geo-environmental indices based on critical parameters/elements (e.g., Ca, Na, PTE, etc.) and the specific requirements of each study (e.g., water use, land use) is preferable. Nonetheless, it is important to recognize that different indices used to assess water suitability for a specific use may occasionally produce contradictory results, potentially leading to incorrect conclusions. According to Tables 4–6, certain indices yield conflicting results regarding the suitability of groundwater samples. While some indices classify all samples as suitable, others consider them entirely unsuitable or unsafe. For instance, the MAR and SAR indices, both used to evaluate irrigation suitability, produce opposing conclusions: the MAR index indicates that all groundwater samples in the Schinos area are unsuitable for irrigation, whereas the SAR index classifies them as suitable. Similar inconsistencies are also observed with other indices. This discrepancy underscores the need for a thorough hydrogeochemical assessment to ensure accurate and holistic interpretation of the data. In the case of the present study area, the presence of ultramafic rocks significantly influences the MAR index values due to the increased Mg^{2+} groundwater concentrations.

Another limitation is that some geo-environmental indices have values influenced by the relative weight of their parameters (e.g., PIG, WQI) or rely on ideal and/or guideline values (e.g., HPI, NPI, PIG, WQI, etc.), a consideration that impacts the final result of the index and is directly associated with the researcher's experience/knowledge and choices. It is likely that different researchers calculating the same index may obtain varying values due to differences in methodology or parameter weighting, which, in some extreme cases, could lead to different interpretations. Therefore, the most crucial principle in such studies is that the geo-environmental indices should not be prioritized over elemental concentrations. Thus, they serve as tools to highlight water suitability or to compare its quality against certain standards. Additionally, some indices are based on identical or nearly identical calculation methods, making their inclusion redundant and unnecessary for further consideration. Some geo-environmental indices show similar results with only minor variations (e.g., %Na-SSP, WQI-PIG, RI-Cl/HCO₃, MAR-Ca/Mg, etc.). This observation is further reinforced by the individual index results and the statistical analysis, which reveals correlation values close to 1, similar factor loadings in the FA, and low linkage distances in the HCA (Figures 6–8, Table 7). Generally, the application of multivariate statistical methods highlights significant similarities among geo-environmental indices, raising concerns about the necessity of calculating all of them individually and underscoring the importance of focusing on the most meaningful indices to enhance analytical efficiency and provide more targeted, insightful results. It is important to note that a water sample may show excellent quality in terms of major element chemistry, yet still contain elevated levels of PTEs. In such cases, the water might be classified as good or excellent and deemed suitable for drinking and irrigation based solely on its major element concentrations. However, an analysis focusing on PTE-related indices could categorize the same water as poor quality. This highlights the importance of conducting a combined analysis using multiple indices, as recommended by this study, to achieve a more comprehensive and accurate assessment of water quality and its suitability for various uses. For instance, coupling two geo-environmental indices with different objectives can yield critical insights into chemometric analysis and water use, ultimately enhancing groundwater management.

This clustering effect stems from the significant influence certain elements exert on the final index values. While each index is typically assessed separately, combining indices from different categories allows for a more robust evaluation of groundwater quality. For example, Figure 9 illustrates a bivariate plot of the WQI, which assesses water suitability for drinking, alongside the HPI, which evaluates water quality based on the occurrence of PTEs. This integrated approach creates six distinct sub-fields, enabling the classification of samples based on their ability to meet both criteria for good water quality. By merging these indices, the assessment of groundwater quality is significantly enhanced, offering a more comprehensive understanding compared to the use of individual indices alone. For example, the coupling of WQI and HPI revealed that 64.7% of the samples fall into the excellent and suitable category, 11.8% into the good and suitable category, 1.47% into the poor and suitable category, 2.94% into the excellent and unsuitable category, 16.2% into the good and unsuitable category, and 2.94% into the poor and unsuitable category. All samples from the Loutraki area and the Gerania Mts. are classified as having excellent water quality based on WQI, with only one sample from the Loutraki area deemed unsuitable according to HPI. In contrast, the majority of samples from the Schinos area exhibit lower water quality when evaluated using both WQI and HPI results (Figure 9).
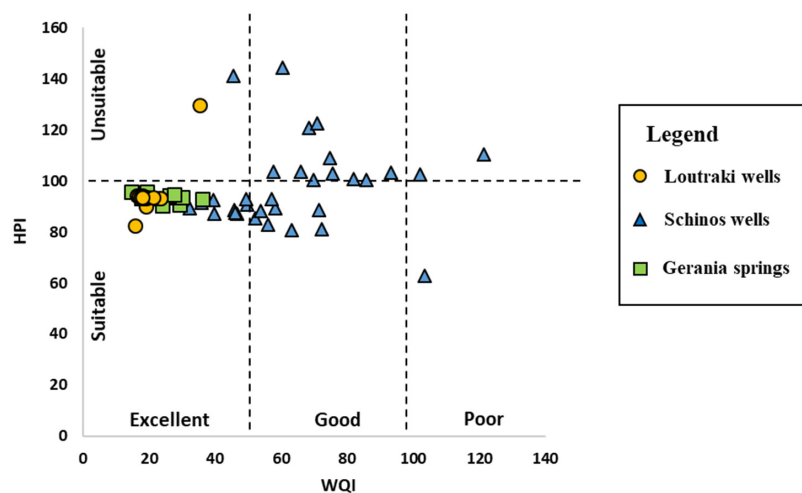

Figure 9. Cross-plot of WQI vs. HPI for the 68 groundwater samples from the Loutraki–Schinos–Gerania Mts. Region.

The combined analysis of ionic ratios is a valuable tool for understanding the occurrence, mobility, and transport of PTEs in the environment. In this investigation, the methodology of Papazotos et al. [21], used to distinguish the sources of PTEs, was followed, an approach that was first applied to various PTEs in the Psachna Basin, Euboea, Greece. Figures 10 and 11 display several ionic ratio diagrams that illustrate the dominant hydrochemical processes in the study area. Figure 10a presents the Cl/HCO_3–Cl and Cl/HCO_3–HCO_3 ratio diagrams for the Loutraki–Schinos–Gerania Mts. region. The majority of the groundwater samples from the study area are plotted in the 'carbonate dissolution' field, indicating that groundwater recharge is the dominant hydrogeological process. However, some samples exhibit a molar ratio greater than 0.5 (and in several cases, >1), reflecting the influence of seawater intrusion in certain parts of the study area. Figure 10b presents the Si/NO_3–Si and Si/NO_3–NO_3 ratio diagrams for the Loutraki–Schinos–Gerania Mts. region. Most groundwater samples fall within the 'silicate dissolution' field, while some from the Schinos area are plotted in the 'nitrate pollution' field. Samples outside these two ranges may be influenced by other factors, such as carbonate mineral dissolution, as indicated in Figure 10a. It is important to emphasize that, in any case, the coexistence of

geogenic and anthropogenic activities (such as agricultural practices, sewage discharges, etc.) cannot be ruled out. However, this should be further investigated by analyzing the complete dataset and other qualitative criteria. The concentration of chemical elements is a crucial indicator in environmental geochemical research and should be carefully considered. Neglecting these concentrations can lead to misleading results, as focusing solely on molar ratios may not provide the desired information. For instance, areas unaffected by human activities typically exhibit NO_{3-} concentrations below 10 mg/L [50]. Therefore, NO_{3-} concentrations below 0.16 mmol/L should not be attributed to anthropogenic influences, regardless of the Si/NO_3 molar ratio. Conversely, a high or very high Si/NO_3 molar ratio accompanied by low Si concentrations should not be attributed to the dissolution of silicate minerals but rather to other natural factors, such as the dissolution of carbonates, or the influence of seawater or rainwater.
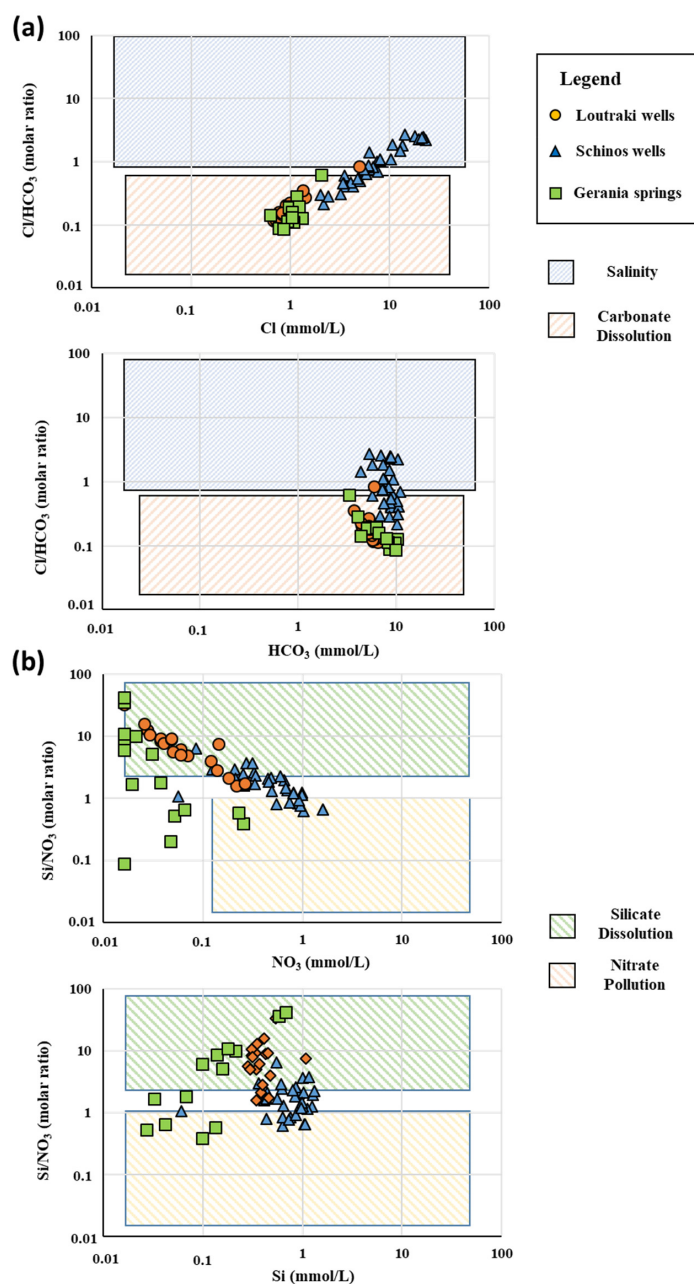

Figure 10. Bivariate diagrams of (**a**) Cl/HCO_3 (molar ratio) vs. Cl (mmol/L) and Cl/HCO_3 (molar ratio) vs. HCO_3 (mmol/L) and (**b**) Si/NO_3 (molar ratio) vs. NO_3 (mmol/L) and Si/NO_3 (molar ratio) vs. Si (mmol/L) for the 68 groundwater samples from the Loutraki–Schinos–Gerania Mts. region.
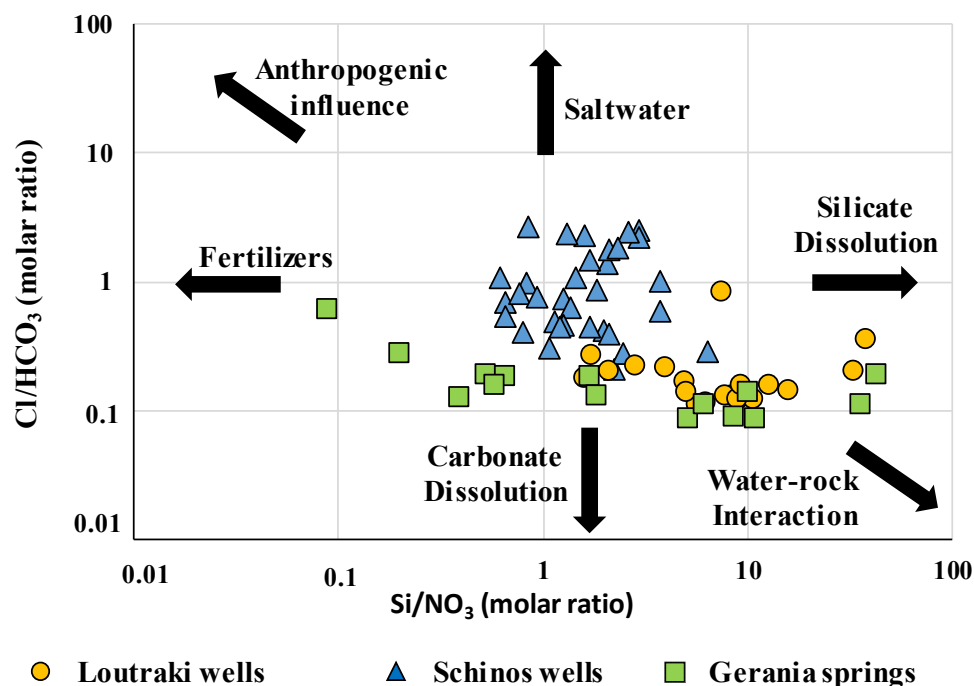
Figure 11. Evaluation of major hydrogeochemical processes affecting water chemistry using Cl/HCO$_3$ vs. Si/NO$_3$ diagram.

Finally, combining the information presented, the coupling of the two molar ratios (Cl/HCO$_3$ and Si/NO$_3$) can provide valuable insights into the groundwater geochemistry of a complex aquifer system. This approach accounts for processes such as seawater intrusion, agricultural activities, and water–rock/soil interactions, including the involvement of both carbonate and silicate mineral phases (Figure 11). As shown in Figure 11, the samples from the springs of the Gerania Mt. area are characterized by relatively stable Cl/HCO$_3$ ionic ratios and varying Si/NO$_3$ ionic ratios. However, the co-evaluation with the diagrams that contain ionic ratios and elemental concentrations (Figure 10) indicates the dominance of geogenic factors in groundwater quality. The same pattern is observed in the samples from the Loutraki area, without the same variability. In contrast, the samples from the Schinos area exhibit an upward and leftward trend, likely due to seawater intrusion and human activities, which contribute to the degradation of the aquifer table.

The high salinity caused by seawater intrusion into the groundwater is linked to the elevated As concentrations observed in the study area, as concentrations tend to increase in the central and upper parts of the plot of Figure 12a. Multivariate statistical analyses (e.g., FA, HCA) and correlation coefficients from our previous study [30] have revealed a statistical association between As and major/trace elements commonly found in seawater, such as Cl$^-$, Br, and Li. In contrast, Cr exhibits a different pattern, with low to high concentrations trending from the center to the left of the diagram (Figure 12b). The category with the highest Cr concentrations (>Q3) is dominated by low Si/NO$_3$ ratios, suggesting that agricultural activities are the primary source of Cr. Multivariate statistical analyses (e.g., FA, HCA), correlation coefficients, and spatial distribution maps from other studies [30,89,126–128] further support the role of fertilization in Cr mobilization in the environment. Thus, coupling ionic ratios can reveal valuable insights into PTE geochemistry, and environmental geoscientists are increasingly recommending the use of these tools in their research.
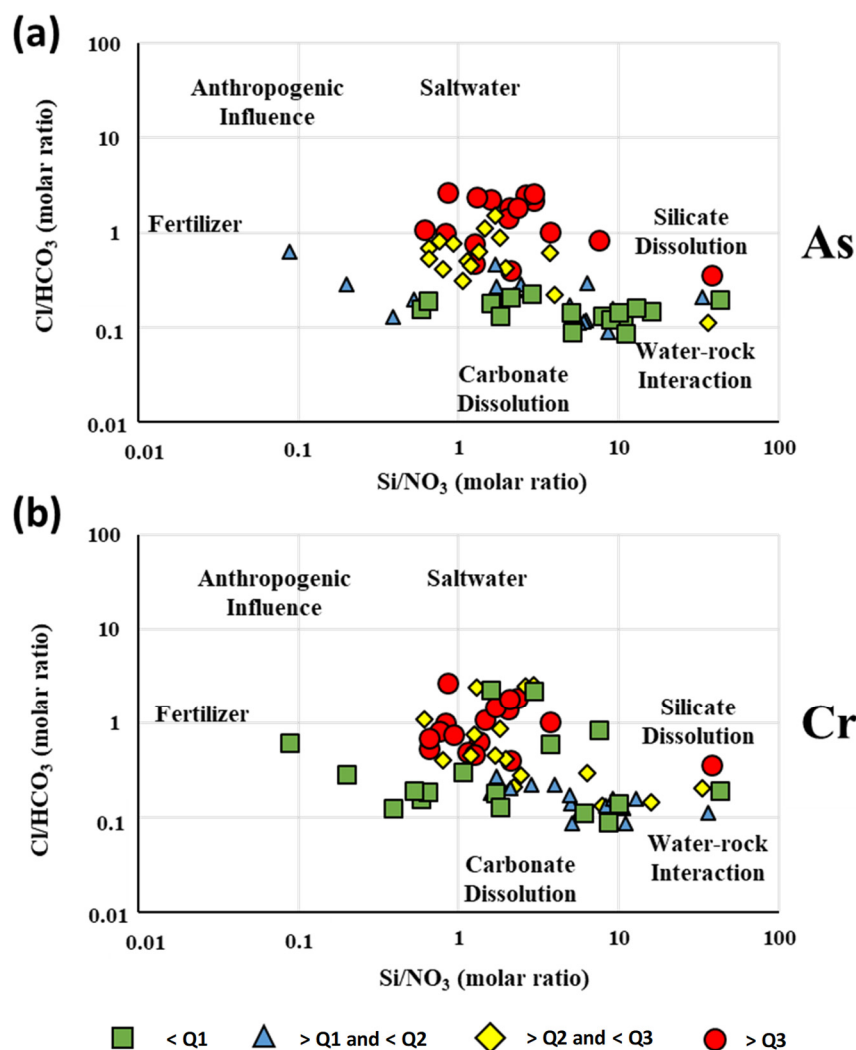
Figure 12. Bivariate Cl/HCO$_3$ vs. Si/NO$_3$ diagrams of (**a**) As, and (**b**) Cr (Q1: first quartile; Q2: second quartile or median; Q3: third quartile).

This study suggests the development of a novel more comprehensive geo-environmental index to enhance the accuracy and effectiveness of environmental research. Such an index would integrate both quantitative data, such as concentrations of chemical elements, and qualitative factors, including land use, geology, hydrogeology, and key physicochemical parameters (e.g., pH, Eh, and DO). Future research is encouraged to integrate both qualitative and quantitative groundwater data within this geo-environmental framework, leveraging ML and deep learning (DL) techniques to develop the new index for optimal water quality assessment and management. Furthermore, it is important to note that the new geo-environmental index should replace the outdated and misrepresentation term 'heavy metals' ([129–131]) with the modern term 'potentially toxic elements' [121,129]; the established widely used geo-environmental indices require modernization such as HEI and HPI.

This study does not merely offer another groundwater suitability and quality assessment for a study area. It stands apart from other published works by, for the first time, providing a comprehensive exploration of the critical role of geo-environmental indices. The paper offers a detailed evaluation of the strengths and weaknesses of these methodologies and presents specific recommendations for their optimal application, highlighting the novel contributions of this research. Assessing geo-environmental indices and optimizing their application in environmental science can enhance sustainable groundwater

management practices and support the achievement of Sustainable Development Goal 6 (SDG-6), particularly in mitigating groundwater pollution. By systematically evaluating geo-environmental indices, pollution sources can be identified, and targeted strategies can be developed to improve water quality, ensuring safe water resources for current and future generations.

4. Conclusions

This paper evaluates the groundwater quality of the NE Peloponnese for various uses by employing geo-environmental indices and ionic ratios. For the first time, data from 68 groundwater samples previously collected in the study area by Papazotos et al. [30] were utilized to calculate these indices and ratios. The analysis also incorporated geological, hydrogeological, geochemical, land/water use, and mineralogical information, applying both classical and multivariate statistical methods. The main findings of this research are summarized as follows:

- Most groundwater samples from the study area are suitable for irrigation purposes. However, some samples from the Schinos area exhibit medium quality due to elevated concentrations of NO_{3-}, Cl^-, and Na^+. This degradation in water quality is primarily attributed to relatively limited anthropogenic influences on the environment (e.g., small-scale farming, irrigation, low-impact tourism), including the use of septic tanks and fertilizer application, as well as seawater intrusion.
- All samples from the Loutraki area and the Gerania Mts. demonstrate good quality for drinking water. In the Schinos area, while some samples maintain good water quality, others are classified as medium to poor.
- Most samples exhibit good quality regarding PTE concentrations. However, elevated concentrations of Cr and As were detected in some samples from the Loutraki and Schinos areas.
- Based on all indices assessing groundwater suitability for drinking, irrigation, and PTE load, water samples from the Loutraki area and the Gerania Mts. exhibit good to excellent quality, whereas the Schinos area shows comparatively poorer groundwater quality.
- Statistical analysis identified distinct groups of geo-environmental indices based on dominant parameters, suggesting that focusing on the most significant indices can enhance the clarity and relevance of the analysis, reduce redundancy, and improve interpretability, ultimately emphasizing the need for a more robust and systematic methodological framework for assessing groundwater quality rather than relying on numerous geo-environmental indices.
- Some geo-environmental indices designed to evaluate similar water uses yield conflicting results. This issue arises because elemental concentrations are a more critical determinant of water quality than the indices themselves.
- All geo-environmental indices, influenced by parameter weighting (e.g., WQI, HPI, IWQI, etc.), produce results that vary with the researcher's experience/knowledge and methodology, leading to potential differences in interpretation. To minimize inaccuracies in data interpretation, a more robust and standardized scientific approach is required.
- Coupling geo-environmental indices significantly enhances the comprehensive interpretation and evaluation of groundwater quality, optimizing groundwater management.
- Coupling ionic ratios proved valuable in determining the occurrence and mobility of PTEs in the environment. This approach was effectively applied to evaluate As and Cr concentrations in NE Peloponnese, Greece (study area).

In conclusion, further research is recommended to establish regulations governing water use, informed by both usage patterns and epidemiological studies. This research would support policymakers in using multiple-criteria decision analysis (MCDA) and enable stakeholders to enhance public health while optimizing water resource management. Furthermore, this study provides a comprehensive guide for researchers by consolidating the geo-environmental indices used in groundwater quality suitability and hydrogeochemical evaluation. The strategic integration of geo-environmental indices with data from other scientific disciplines (e.g., medicine, biology, chemistry, etc.), could significantly advance environmental sustainability and contribute to achieving the SDGs.

References

1. Priyan, K. Issues and Challenges of Groundwater and Surface Water Management in Semi-Arid Regions. In *Groundwater Resources Development and Planning in the Semi-Arid Region*; Springer: Berlin/Heidelberg, Germany, 2021.
2. Scanlon, B.R.; Fakhreddine, S.; Rateb, A.; de Graaf, I.; Famiglietti, J.; Gleeson, T.; Grafton, R.Q.; Jobbagy, E.; Kebede, S.; Kolusu, S.R.; et al. Global Water Resources and the Role of Groundwater in a Resilient Water Future. *Nat. Rev. Earth Environ.* **2023**, *4*, 87–101. [CrossRef]
3. Qadir, M.; Sharma, B.R.; Bruggeman, A.; Choukr-Allah, R.; Karajeh, F. Non-Conventional Water Resources and Opportunities for Water Augmentation to Achieve Food Security in Water Scarce Countries. *Agric. Water Manag.* **2007**, *87*, 2–22. [CrossRef]
4. Brindha, K.; Schneider, M. Impact of Urbanization on Groundwater Quality. *GIS Geostat. Tech. Groundw. Sci.* **2019**, *2019*, 179–196.
5. Chowdhary, P.; Bharagava, R.N.; Mishra, S.; Khan, N. Role of Industries in Water Scarcity and Its Adverse Effects on Environment and Human Health. In *Environmental Concerns and Sustainable Development*; Springer: Berlin/Heidelberg, Germany, 2020.
6. Lall, U.; Josset, L.; Russo, T. A Snapshot of the World's Groundwater Challenges. *Annu. Rev. Environ. Resour.* **2020**, *45*, 171–194. [CrossRef]
7. Mukherjee, A.; Scanlon, B.R.; Aureli, A.; Langan, S.; Guo, H.; McKenzie, A. Global Groundwater: From Scarcity to Security through Sustainability and Solutions. In *Global Groundwater: Source, Scarcity, Sustainability, Security, and Solutions*; Elsevier: Amsterdam, The Netherlands, 2020.
8. Sharma, R.; Kumar, R.; Agrawal, P.R.; Ittishree; Chankit; Gupta, G. Groundwater Extractions and Climate Change. In *Water Conservation in the Era of Global Climate Change*; Elsevier: Amsterdam, The Netherlands, 2021.
9. Makanda, K.; Nzama, S.; Kanyerere, T. Assessing the Role of Water Resources Protection Practice for Sustainable Water Resources Management: A Review. *Water* **2022**, *14*, 3153. [CrossRef]
10. Chakraborty, T.K.; Islam, M.S.; Ghosh, G.C.; Ghosh, P.; Zaman, S.; Habib, A.; Hossain, M.R.; Bosu, H.; Islam, M.R.; Al Imran, M.; et al. Human Health Risk and Hydro-Geochemical Appraisal of Groundwater in the Southwest Part of Bangladesh Using GIS, Water Quality Indices, and Multivariate Statistical Approaches. *Toxin Rev.* **2023**, *42*, 285–299. [CrossRef]
11. Arumugam, T.; Kinattinkara, S.; Kannithottathil, S.; Velusamy, S.; Krishna, M.; Shanmugamoorthy, M.; Sivakumar, V.; Boobalakrishnan, K.V. Comparative Assessment of Groundwater Quality Indices of Kannur District, Kerala, India Using Multivariate Statistical Approaches and GIS. *Environ. Monit. Assess.* **2023**, *195*, 29. [CrossRef] [PubMed]
12. Kazapoe, R.W.; Addai, M.O.; Amuah, E.E.Y.; Dankwa, P. Hydrogeochemical Characterization of Groundwater in the Wassa Amenfi East and Prestea-Huni Valley Areas of Southern Ghana Using GIS-Based and Multivariate Statistical Techniques. *Sustain. Water Resour. Manag.* **2023**, *9*, 141. [CrossRef]

13. Benyoussef, S.; Arabi, M.; El Yousfi, Y.; Makkaoui, M.; Gueddari, H.; El Ouarghi, H.; Abdaoui, A.; Ghalit, M.; Zegzouti, Y.F.; Azirar, M.; et al. Assessment of Groundwater Quality Using Hydrochemical Process, GIS and Multivariate Statistical Analysis at Central Rif, North Morocco. *Environ. Earth Sci.* **2024**, *83*, 515. [CrossRef]

14. Singh, G.; Singh, J.; Wani, O.A.; Egbueri, J.C.; Agbasi, J.C. Assessment of Groundwater Suitability for Sustainable Irrigation: A Comprehensive Study Using Indexical, Statistical, and Machine Learning Approaches. *Groundw. Sustain. Dev.* **2024**, *24*, 101059. [CrossRef]

15. Egbueri, J.C.; Agbasi, J.C. Data-Driven Soft Computing Modeling of Groundwater Quality Parameters in Southeast Nigeria: Comparing the Performances of Different Algorithms. *Environ. Sci. Pollut. Res.* **2022**, *29*, 38346–38373. [CrossRef] [PubMed]

16. Haggerty, R.; Sun, J.; Yu, H.; Li, Y. Application of Machine Learning in Groundwater Quality Modeling—A Comprehensive Review. *Water Res.* **2023**, *233*, 119745. [CrossRef]

17. Vasileiou, E.; Papazotos, P.; Dimitrakopoulos, D.; Perraki, M. Expounding the Origin of Chromium in Groundwater of the Sarigkiol Basin, Western Macedonia, Greece: A Cohesive Statistical Approach and Hydrochemical Study. *Environ. Monit. Assess.* **2019**, *191*, 509. [CrossRef]

18. Quino-Lima, I.; Ramos-Ramos, O.; Ormachea-Muñoz, M.; Quintanilla-Aguirre, J.; Duwig, C.; Maity, J.P.; Sracek, O.; Bhattacharya, P. Spatial Dependency of Arsenic, Antimony, Boron and Other Trace Elements in the Shallow Groundwater Systems of the Lower Katari Basin, Bolivian Altiplano. *Sci. Total Environ.* **2020**, *719*, 137505. [CrossRef]

19. Ijumulana, J.; Ligate, F.; Bhattacharya, P.; Mtalo, F.; Zhang, C. Spatial Analysis and GIS Mapping of Regional Hotspots and Potential Health Risk of Fluoride Concentrations in Groundwater of Northern Tanzania. *Sci. Total Environ.* **2020**, *735*, 139584. [CrossRef]

20. Verma, P.; Singh, P.K.; Sinha, R.R.; Tiwari, A.K. Assessment of Groundwater Quality Status by Using Water Quality Index (WQI) and Geographic Information System (GIS) Approaches: A Case Study of the Bokaro District, India. *Appl. Water Sci.* **2020**, *10*, 27. [CrossRef]

21. Papazotos, P.; Vasileiou, E.; Vasilakis, S.; Perraki, M. A Novel Hydrogeochemical Approach to Delineate the Origin of Potentially Toxic Elements in Groundwater: Sophisticated Molar Ratios as Environmental Tracers. *Environ. Sci. Pollut. Res.* **2023**, *30*, 74771–74790. [CrossRef]

22. Nwankwoala, H.O.; Okujagu, D.C.; Bolaji, T.A.; Papazotos, P.G.; Ugbenna, K.G. Assessment of Groundwater Quality for Irrigation Suitability: A Case Study of Khana and Gokana LGAs, Rivers State, Nigeria. *Environ. Earth Sci.* **2023**, *82*, 292. [CrossRef]

23. Kumar, M.; Kumari, K.; Ramanathan, A.; Saxena, R. A Comparative Evaluation of Groundwater Suitability for Irrigation and Drinking Purposes in Two Intensively Cultivated Districts of Punjab, India. *Environ. Geol.* **2007**, *53*, 553–574. [CrossRef]

24. Karunanidhi, D.; Aravinthasamy, P.; Deepali, M.; Subramani, T.; Bellows, B.C.; Li, P. Groundwater Quality Evolution Based on Geochemical Modeling and Aptness Testing for Ingestion Using Entropy Water Quality and Total Hazard Indexes in an Urban-Industrial Area (Tiruppur) of Southern India. *Environ. Sci. Pollut. Res.* **2021**, *28*, 18523–18538. [CrossRef]

25. Stamatis, G.; Parpodis, K.; Filintas, A.; Zagana, E. Groundwater Quality, Nitrate Pollution and Irrigation Environmental Management in the Neogene Sediments of an Agricultural Region in Central Thessaly (Greece). *Environ. Earth Sci.* **2011**, *64*, 1081–1105. [CrossRef]

26. Papazotos, P.; Koumantakis, I.; Vasileiou, E. Hydrogeochemical Assessment and Suitability of Groundwater in a Typical Mediterranean Coastal Area: A Case Study of the Marathon Basin, NE Attica, Greece. *HydroResearch* **2019**, *2*, 49–59. [CrossRef]

27. Panagopoulos, G.; Lambrakis, N.; Chalvantzis, C.; Bekiari, V.; Avramidis, P. Assessing the suitability of groundwater for drinking and agricultural uses in the zacharo basin, sw peloponnesus. *Bull. Geol. Soc. Greece* **2017**, *50*, 899–906. [CrossRef]

28. Papadopoulos, K.; Lappas, I. Groundwater quality degradation due to Cr6+ presence in Schinos area, prefecture of Corinth, Central Greece. In Proceedings of the 10th International Hydrogeological Congress of Greece, Thessaloniki, Greece, 8–10 October 2014.

29. Pyrgaki, K.; Argyraki, A.; Kelepertzis, E.; Paraskevopoulou, V.; Botsou, F.; Dassenakis, E.; Mitsis, I.; Skourtsos, E. Occurence of Hexavalent Chromium in the Ophiolite Related Aquifers of Loytraki and Schinos Areas. *Bull. Geol. Soc. Greece* **2017**, *50*, 2261–2270. [CrossRef]

30. Papazotos, P.; Vasileiou, E.; Perraki, M. Elevated Groundwater Concentrations of Arsenic and Chromium in Ultramafic Environments Controlled by Seawater Intrusion, the Nitrogen Cycle, and Anthropogenic Activities: The Case of the Gerania Mountains, NE Peloponnese, Greece. *Appl. Geochem.* **2020**, *121*, 104697. [CrossRef]

31. Pyrgaki, K.; Argyraki, A.; Botsou, F.; Kelepertzis, E.; Paraskevopoulou, V.; Karavoltsos, S.; Mitsis, I.; Dassenakis, E. Hydrogeochemical Investigation of Cr in the Ultramafic Rock-Related Water Bodies of Loutraki Basin, Northeast Peloponnese, Greece. *Env. Earth Sci.* **2021**, *80*, 62. [CrossRef]

32. Kelepertzis, E.; Pyrgaki, K.; Argyraki, A.; Botsou, F.; Boeckx, P.; Karavoltsos, S.; Dassenakis, M. Application of Dual Isotopes (δ 15 N, δ 18 O) to Determine Nitrate Contamination Sources in Cr(VI)-Impacted Groundwater of Central Greece Aquifers. In Proceedings of the 15th International Congress of the Geological Society of Greece Athens, Athens, Greece, 22–24 May 2019.

33. Pyrgaki, K.; Kelepertzis, E.; Argyraki, A.; Boeckx, P.; Botsou, F.; Dassenakis, E. Identification of Sources and Transformations of Nitrate in Cr(VI)-Impacted Alluvial Aquifers by a Hydrogeochemical and Δ15N-NO3− and Δ18O-NO3− Isotopes Approach. *Environ. Sci. Pollut. Res.* **2022**, *29*, 57703–57719. [CrossRef] [PubMed]

34. Bornovas, J.; Eleutheriou, A.; Gaitanakis, P. 1970. Geological Map of Greece, 1: 50000, Kaparellion Sheet, IGME.

35. Bornovas, J.; Lalechos, N.; Filippakis, N. 1970. Geological Map of Greece, 1:50000, Korinthos Sheet, IGME.

36. Bornovas, J.; Lalechos, N.; Filippakis, N. *Geological Map of Greece, 1:50000, Korinthos Sheet*; Institute of Geology and Mineral Exploration (IGME): Athens, Greece, 1969.

37. Voudouris, K.; Stamatis, G. Distribution and Fractal Analysis of Parameters of the Upper Part of Unsaturated Zone of the Alluvial Aquifer of Loutraki Basin. *Min. Metall. Ann.* **2002**, *12*, 39–54.

38. Pyrgaki, K.; Argyraki, A.; Kelepertzis, E.; Botsou, F.; Megremi, I.; Karavoltsos, S.; Dassenakis, E.; Mpouras, T.; Dermatas, D. A DPSIR Approach to Selected Cr(VI) Impacted Groundwater Bodies of Central Greece. *Bull. Environ. Contam. Toxicol.* **2021**, *106*, 446–452. [CrossRef] [PubMed]

39. Stamatis, G.; Voudouris, K. Delineation of Protection Zones According to Hydrogeological Criteria: The Case Study of Loutraki Alluvial Aquifer. *Miner. Wealth* **2000**, *2000*, 13–36.

40. Dotsika, E.; Poutoukis, D.; Raco, B. Fluid Geochemistry of the Methana Peninsula and Loutraki Geothermal Area, Greece. *J. Geochem. Explor.* **2010**, *104*, 97–104. [CrossRef]

41. D'Alessandro, W.; Calabrese, S.; Bellomo, S.; Brusca, L.; Daskalopoulou, K.; Li Vigni, L.; Randazzo, L.; Kyriakopoulos, K. Impact of Hydrothermal Alteration Processes on Element Mobility and Potential Environmental Implications at the Sousaki Solfataric Field (Corinthia—Greece). *J. Volcanol. Geotherm. Res.* **2020**, *407*, 107121. [CrossRef]

42. Giannakopoulou, P.P.; Petrounias, P.; Rogkala, A.; Tsikouras, B.; Stamatis, P.M.; Pomonis, P.; Hatzipanagiotou, K. The Influence of the Mineralogical Composition of Ultramafic Rocks on Their Engineering Performance: A Case Study from the Veria-Naousa and Gerania Ophiolite Complexes (Greece). *Geosciences* **2018**, *8*, 251. [CrossRef]

43. Vassilakis, E.; Royden, L.; Papanikolaou, D. Kinematic Links between Subduction along the Hellenic Trench and Extension in the Gulf of Corinth, Greece: A Multidisciplinary Analysis. *Earth Planet. Sci. Lett.* **2011**, *303*, 108–120. [CrossRef]

44. Kaplanis, A.; Koukouvelas, I.; Xypolias, P.; Kokkalas, S. Kinematics and Ophiolite Obduction in the Gerania and Helicon Mountains, Central Greece. *Tectonophysics* **2013**, *595–596*, 215–234. [CrossRef]

45. ELSTAT (2021). Hellenic Statistical Authority. Available online: https://www.statistics.gr/en/home (accessed on 15 October 2024).

46. HNMS. Available online: https://emy.gr/hnms-stations (accessed on 20 October 2024).

47. European Environment Agency (EEA) CORINE Land Cover (CLC) 2018, Version 2020_20u1. Derived by Integrating the Data of Land Cover Changes between the Years 2012–2018 (Available at: CLC 2018—Copernicus Land Monitoring Service). Available online: https://land.copernicus.eu/en/products/corine-land-cover/clc2018 (accessed on 20 October 2024).

48. *UNE-EN ISO/IEC/17025:2005*; General Requirements for the Competence of Testing and Calibration Laboratories. 2005.

49. Mutewekil, M.; Awawdeh, M.; Abu, F.; Al-Ajlouni, A. An Innovative Nitrate Pollution Index and Multivariate Statistical Investigations of Groundwater Chemical Quality of Umm Rijam Aquifer (B4), North Yarmouk River Basin, Jordan. In *Water Quality Monitoring and Assessment*; InTech: Rijeka, Croatia, 2012.

50. Panno, S.V.; Kelly, W.R.; Martinsek, A.T.; Hackley, K.C. Estimating Background and Threshold Nitrate Concentrations Using Probability Graphs. *Ground Water* **2006**, *44*, 697–709. [CrossRef]

51. Revelle, R. Criteria for Recognition of the Sea Water in Ground-waters. *Eos Trans. Am. Geophys. Union* **1941**, *22*, 593–597. [CrossRef]

52. Subba Rao, N. PIG: A Numerical Index for Dissemination of Groundwater Contamination Zones. *Hydrol. Process* **2012**, *26*, 3344–3350. [CrossRef]

53. Horton, R.K. An Index Number System for Rating Water Quality. *J. Water Pollut. Control Fed.* **1965**, *37*, 300–306.

54. Brown, M.; McClelland, N.I.; Deininger, R.A.; Tozer, R.G. A Water Quality Index: Do We Dare? *Water Sew. Work.* **1970**, *117*, 339–343.

55. Hossain, M.; Patra, P.K. Water Pollution Index—A New Integrated Approach to Rank Water Quality. *Ecol. Indic.* **2020**, *117*, 106668. [CrossRef]

56. Richards, L.A. Diagnosis and Improvement of Saline and Alkali Soils. *Soil Sci.* **1954**, *78*, 154. [CrossRef]

57. Todd, D.K. *Groundwater Hydrology*, 2nd ed.; Wiley: New York, NY, USA, 1980.

58. Kelley, W.P. Permissible Composition and Concentration of Irrigation Water. *Trans. Am. Soc. Civ. Eng.* **1941**, *106*, 849–855. [CrossRef]

59. Kelley, W.P. *Alkali Soils—Their Formation Properties and Reclamation*; Reinhold Publishing Co.: New York, NY, USA, 1951.

60. Wilcox, L.V. *Classification and Use of Irrigation Waters*; United States Department of Agriculture: Washington, DC, USA, 1955.

61. Ayers, R.S.; Westcot, D.W. *Water Quality for Agriculture*; FAO United Nations: Rome, Italy, 1985.

62. Collins, R.; Jenkins, A. The Impact of Agricultural Land Use on Stream Chemistry in the Middle Hills of the Himalayas, Nepal. *J. Hydrol.* **1996**, *185*, 71–86. [CrossRef]

63. Doneen, L.D. The Influence of Crop and Soil on Percolating Waters. In Proceedings of the 1961 Biennial Conference Groundwater Recharge, Berkeley, CA, USA, 26–27 June 1962; pp. 156–163.

64. Doneen, L.D. *Notes on Water Quality in Agriculture*; Department of Water Science and Engineering, University of California: Oakland, CA, USA, 1964.

65. Rawat, K.S.; Singh, S.K.; Gautam, S.K. Assessment of Groundwater Quality for Irrigation Use: A Peninsular Case Study. *Appl. Water Sci.* **2018**, *8*, 233. [CrossRef]

66. Szabolcs, I.; Darab, C. The Influences of Irrigation Water of High Sodium Carbonate Contents on Soils. In Proceedings of the 8th International Congress Soil Science Sodic Soils, Research Institute for Soil Science and Agricultural Chemistry of the Hungarian Academy of Sciences, Izmir, Turkey, 15–17 May 1964; ISSS Trans II: Tsukuba, Japan, 1964; pp. 802–812.

67. Paliwal, K.V. *Irrigation with Saline Water*; Water Technology Centre, Indian Agriculture Research Institute: New Delhi, India, 1972.

68. Hem, J.D. *Study and Interpretation of the Chemical Characteristics of Natural Water*; US Geological Survey Water-Supply Paper; United States Government Printing Office: Washington, DC, USA, 1985; Volume 2254.

69. Giggenbach, W.F. Geothermal Solute Equilibria. Derivation of Na-K-Mg-Ca Geoindicators. *Geochim. Cosmochim. Acta* **1988**, *52*, 2749–2765. [CrossRef]

70. Eaton, F.M. Significance of Carbonates in Irrigation Waters. *Soil Sci.* **1950**, *69*, 123–134. [CrossRef]

71. Boyd, C.E.; Tucker, C.S. *Handbook for Aquaculture Water Quality*; Craftmaster Printers, Inc.: Auburn, AL, USA, 2014.

72. Sengupta, P. Potential Health Impacts of Hard Water. *Int. J. Prev. Med.* **2013**, *4*, 866–875.

73. Sawyer, G.N.; McCarthy, D.L. *Chemistry of Sanitary Engineers*; McGraw Hill: New York, NY, USA, 1967; p. 518.

74. Meireles, A.C.M.; de Andrade, E.M.; Chaves, L.C.G.; Frischkorn, H.; Crisostomo, L.A. A New Proposal of the Classification of Irrigation Water. *Rev. Ciência Agronômica* **2010**, *41*, 349–357. [CrossRef]

75. Mkilima, T. Groundwater Salinity and Irrigation Suitability in Low-Lying Coastal Areas. A Case of Dar Es Salaam, Tanzania. *Watershed Ecol. Environ.* **2023**, *5*, 173–185. [CrossRef]

76. World Health Organization (WHO). *Guidelines for Drinking Water Quality*; WHO: Geneva, Switzerland, 2017.

77. Subramani, T.; Elango, L.; Damodarasamy, S.R. Groundwater Quality and Its Suitability for Drinking and Agricultural Use in Chithar River Basin, Tamil Nadu, India. *Environ. Geol.* **2005**, *47*, 1099–1110. [CrossRef]

78. Dore, M.P.; Parodi, G.; Portoghese, M.; Errigo, A.; Pes, G.M. Water Quality and Mortality from Coronary Artery Disease in Sardinia: A Geospatial Analysis. *Nutrients* **2021**, *13*, 2858. [CrossRef] [PubMed]

79. Backman, B.; Bodiš, D.; Lahermo, P.; Rapant, S.; Tarvainen, T. Application of a Groundwater Contamination Index in Finland and Slovakia. *Environ. Geol.* **1998**, *36*, 55–64. [CrossRef]

80. Edet, A.E.; Offiong, O.E. Evaluation of Water Quality Pollution Indices for Heavy Metal Contamination Monitoring. A Study Case from Akpabuyo-Odukpani Area, Lower Cross River Basin (Southeastern Nigeria). *GeoJournal* **2002**, *57*, 295–304. [CrossRef]

81. Prasanna, M.V.; Praveena, S.M.; Chidambaram, S.; Nagarajan, R.; Elayaraja, A. Evaluation of Water Quality Pollution Indices for Heavy Metal Contamination Monitoring: A Case Study from Curtin Lake, Miri City, East Malaysia. *Environ. Earth Sci.* **2012**, *67*, 1987–2001. [CrossRef]

82. Spearman, C. The Proof and Measurement of Association between Two Things. *Am. J. Psychol.* **1904**, *15*, 72–101. [CrossRef]

83. Evans, J. *Straightforward Statistics for the Behavioral Sciences*; Brooks/Cole Publishing Company: Pacific Grove, CA, USA, 1996.

84. Shrestha, N. Factor Analysis as a Tool for Survey Analysis. *Am. J. Appl. Math. Stat.* **2021**, *9*, 4–11. [CrossRef]

85. Dziuban, C.D.; Shirkey, E.C. When Is a Correlation Matrix Appropriate for Factor Analysis? Some Decision Rules. *Psychol. Bull.* **1974**, *81*, 358–361. [CrossRef]

86. Kaiser, H.F. The Varimax Criterion for Analytic Rotation in Factor Analysis. *Psychometrika* **1958**, *23*, 187–200. [CrossRef]

87. Kaiser, H.F. The Application of Electronic Computers to Factor Analysis. *Educ. Psychol. Meas.* **1960**, *20*, 141–151. [CrossRef]

88. Liu, C.W.; Lin, K.H.; Kuo, Y.M. Application of Factor Analysis in the Assessment of Groundwater Quality in a Blackfoot Disease Area in Taiwan. *Sci. Total Environ.* **2003**, *313*, 77–89. [CrossRef]

89. Papazotos, P.; Vasileiou, E.; Perraki, M. The Synergistic Role of Agricultural Activities in Groundwater Quality in Ultramafic Environments: The Case of the Psachna Basin, Central Euboea, Greece. *Environ. Monit. Assess.* **2019**, *191*, 317. [CrossRef] [PubMed]

90. Kaiser, H.F. A Second Generation Little Jiffy. *Psychometrika* **1970**, *35*, 401–415. [CrossRef]

91. Bartlett, M.S. Tests of Significance in Factor Analysis. *Br. J. Stat. Psychol.* **1950**, *3*, 77–85. [CrossRef]

92. Ward, J.H. Hierarchical Grouping to Optimize an Objective Function. *J. Am. Stat. Assoc.* **1963**, *58*, 236–244. [CrossRef]

93. Meybeck, M. Global Chemical Weathering of Surficial Rocks Estimated from River Dissolved Loads. *Am. J. Sci.* **1987**, *287*, 401–428. [CrossRef]

94. Stamatakis, M.G.; Mitsis, I. The Occurrences of Mg-Hydroxycarbonates in Serpentinites of the Western Section of the South Aegean Volcanic Arc (West Attica Peninsula-Northeastern Argolis Peninsula), Greece. *Bull. Geol. Soc. Greece* **2013**, *47*, 427–437. [CrossRef]

95. Ficklin, W.H.; Plumlee, G.S.; Smith, K.S.; McHugh, J.B. Geochemical Classification of Mine Drainages and Natural Drainages in Mineralized Areas. In Proceedings of the International Symposium on Water-Rock Interaction, Park City, UT, USA, 13–18 July 1992; pp. 381–384.

96. Egbueri, J.C.; Mgbenu, C.N.; Digwo, D.C.; Nnyigide, C.S. A Multi-Criteria Water Quality Evaluation for Human Consumption, Irrigation and Industrial Purposes in Umunya Area, Southeastern Nigeria. *Int. J. Environ. Anal. Chem.* **2023**, *103*, 3351–3375. [CrossRef]

97. Rezaei, A.; Hassani, H.; Jabbari, N. Evaluation of Groundwater Quality and Assessment of Pollution Indices for Heavy Metals in North of Isfahan Province, Iran. *Sustain. Water Resour. Manag.* **2019**, *5*, 491–512. [CrossRef]

98. Bouselsal, B.; Satouh, A.; Egbueri, J.C. Evaluating Water Quality, Mineralization Mechanisms, and Potential Health Risks of Nitrate Contamination in the Continental Intercalaire Aquifer of Reggane, Algeria. *Environ. Earth Sci.* **2024**, *83*, 539. [CrossRef]

99. El Mountassir, O.; Bahir, M.; Ouazar, D.; Chehbouni, A.; Carreira, P.M. Temporal and Spatial Assessment of Groundwater Contamination with Nitrate Using Nitrate Pollution Index (NPI), Groundwater Pollution Index (GPI), and GIS (Case Study: Essaouira Basin, Morocco). *Environ. Sci. Pollut. Res.* **2022**, *29*, 17132–17149. [CrossRef] [PubMed]

100. Sanad, H.; Mouhir, L.; Zouahri, A.; Moussadek, R.; El Azhari, H.; Yachou, H.; Ghanimi, A.; Oueld Lhaj, M.; Dakak, H. Assessment of Groundwater Quality Using the Pollution Index of Groundwater (PIG), Nitrate Pollution Index (NPI), Water Quality Index (WQI), Multivariate Statistical Analysis (MSA), and GIS Approaches: A Case Study of the Mnasra Region, Gharb Plain, Morocco. *Water* **2024**, *16*, 1263. [CrossRef]

101. Demelash, A.; Atlabachew, A.; Jothimani, M.; Abebe, A. Hydrogeochemical Characterization and Appraisal of Groundwater Quality in Yisr River Catchment, Blue Nile River Basin, Ethiopia, by Using the GIS, WQI, and Statistical Techniques. *J. Chem.* **2023**, *2023*, 8199000. [CrossRef]

102. Witkowski, A.J.; Dąbrowska, D.; Wróbel, J. Groundwater Quality Assessment in the Area of the Zinc Smelter in Miasteczko Śląskie (Poland) Using Selected Metal Indices. *Water* **2024**, *16*, 279. [CrossRef]

103. Abou Zakhem, B.; Hafez, R. Heavy Metal Pollution Index for Groundwater Quality Assessment in Damascus Oasis, Syria. *Environ. Earth Sci.* **2015**, *73*, 6591–6600. [CrossRef]

104. Zhang, Q.; Qian, H.; Xu, P.; Hou, K.; Yang, F. Groundwater Quality Assessment Using a New Integrated-Weight Water Quality Index (IWQI) and Driver Analysis in the Jiaokou Irrigation District, China. *Ecotoxicol. Environ. Saf.* **2021**, *212*, 111992. [CrossRef] [PubMed]

105. Batarseh, M.; Imreizeeq, E.; Tilev, S.; Al Alaween, M.; Suleiman, W.; Al Remeithi, A.M.; Al Tamimi, M.K.; Al Alawneh, M. Assessment of Groundwater Quality for Irrigation in the Arid Regions Using Irrigation Water Quality Index (IWQI) and GIS-Zoning Maps: Case Study from Abu Dhabi Emirate, UAE. *Groundw. Sustain. Dev.* **2021**, *14*, 100611. [CrossRef]

106. Varol, S.; Davraz, A. Evaluation of the Groundwater Quality with WQI (Water Quality Index) and Multivariate Analysis: A Case Study of the Tefenni Plain (Burdur/Turkey). *Environ. Earth Sci.* **2015**, *73*, 1725–1744. [CrossRef]

107. Chaurasia, A.K.; Pandey, H.K.; Tiwari, S.K.; Prakash, R.; Pandey, P.; Ram, A. Groundwater Quality Assessment Using Water Quality Index (WQI) in Parts of Varanasi District, Uttar Pradesh, India. *J. Geol. Soc. India* **2018**, *92*, 76–82. [CrossRef]

108. Panneerselvam, B.; Karuppannan, S.; Muniraj, K. Evaluation of Drinking and Irrigation Suitability of Groundwater with Special Emphasizing the Health Risk Posed by Nitrate Contamination Using Nitrate Pollution Index (NPI) and Human Health Risk Assessment (HHRA). *Hum. Ecol. Risk Assess.* **2020**, *27*, 1324–1348. [CrossRef]

109. Jahan, S.; Strezov, V. Water Quality Assessment of Australian Ports Using Water Quality Evaluation Indices. *PLoS ONE* **2017**, *12*, e0189284. [CrossRef] [PubMed]

110. Pascual Aguilar, J.A.; Campo, J.; Meneu, S.N.; Gimeno-García, E.; Andreu, V. Analysis of Existing Water Information for the Applicability of Water Quality Indices in the Fluvial-Littoral Area of Turia and Jucar Rivers, Valencia, Spain. *Appl. Geogr.* **2019**, *111*, 102062. [CrossRef]

111. Al-Aizari, H.S.; Aslaou, F.; Al-Aizari, A.R.; Al-Odayni, A.B.; Al-Aizari, A.J.M. Evaluation of Groundwater Quality and Contamination Using the Groundwater Pollution Index (GPI), Nitrate Pollution Index (NPI), and GIS. *Water* **2023**, *15*, 3701. [CrossRef]

112. Bahrami, M.; Zarei, A.R.; Rostami, F. Temporal and Spatial Assessment of Groundwater Contamination with Nitrate by Nitrate Pollution Index (NPI) and GIS (Case Study: Fasarud Plain, Southern Iran). *Environ. Geochem. Health* **2020**, *42*, 3119–3130. [CrossRef] [PubMed]

113. Boualem, B.; Egbueri, J.C. Graphical, Statistical and Index-Based Techniques Integrated for Identifying the Hydrochemical Fingerprints and Groundwater Quality of In Salah, Algerian Sahara. *Environ. Geochem. Health* **2024**, *46*, 158. [CrossRef] [PubMed]

114. Ravindra, B.; Subba Rao, N.; Dhanamjaya Rao, E.N. Groundwater Quality Monitoring for Assessment of Pollution Levels and Potability Using WPI and WQI Methods from a Part of Guntur District, Andhra Pradesh, India. *Environ. Dev. Sustain.* **2023**, *25*, 14785–14815. [CrossRef]

115. Shooshtarian, M.R.; Dehghani, M.; Margherita, F.; Gea, O.C.; Mortezazadeh, S. Land Use Change and Conversion Effects on Ground Water Quality Trends: An Integration of Land Change Modeler in GIS and a New Ground Water Quality Index Developed by Fuzzy Multi-Criteria Group Decision-Making Models. *Food Chem. Toxicol.* **2018**, *114*, 204–214. [CrossRef] [PubMed]

116. Kumar, A.; Krishna, A.P. Groundwater Quality Assessment Using Geospatial Technique Based Water Quality Index (WQI) Approach in a Coal Mining Region of India. *Arab. J. Geosci.* **2021**, *14*, 1126. [CrossRef]

117. Abugu, H.O.; Egbueri, J.C.; Agbasi, J.C.; Ezugwu, A.L.; Omeka, M.E.; Ucheana, I.A.; Aralu, C.C. Hydrochemical Characterization of Ground and Surface Water for Irrigation Application in Nigeria: A Review of Progress. *Chem. Afr.* **2024**, *7*, 3011–3036. [CrossRef]

118. Petropoulou, I.; Frousiou, M.-S.; Vasileiou, E. An Overview of Quality Assessment Methods for Water and Soil in Mining Regions. *Mater. Proc.* **2023**, *15*, 31. [CrossRef]

119. Arifullah; Changsheng, H.; Akram, W.; Rashid, A.; Ullah, Z.; Shah, M.; Alrefaei, A.F.; Kamel, M.; Aleya, L.; Abdel-Daim, M.M. Quality Assessment of Groundwater Based on Geochemical Modelling and Water Quality Index (WQI). *Water* **2022**, *14*, 3888. [CrossRef]

120. Bouteraa, O.; Mebarki, A.; Bouaicha, F.; Nouaceur, Z.; Laignel, B. Groundwater Quality Assessment Using Multivariate Analysis, Geostatistical Modeling, and Water Quality Index (WQI): A Case of Study in the Boumerzoug-El Khroub Valley of Northeast Algeria. *Acta Geochim.* **2019**, *38*, 796–814. [CrossRef]

121. Papazotos, P. Potentially Toxic Elements in Groundwater: A Hotspot Research Topic in Environmental Science and Pollution Research. *Environ. Sci. Pollut. Res.* **2021**, *28*, 47825–47837. [CrossRef] [PubMed]

122. Shaw, S.K.; Sharma, A. Assessment of Groundwater Quality and Suitability for Irrigation Purpose Using Irrigation Indices, Remote Sensing and GIS Approach. *Groundw. Sustain. Dev.* **2024**, *26*, 101297. [CrossRef]

123. Khan, R.A.; Khan, N.A.; El Morabet, R.; Alsubih, M.; Qadir, A.; Bokhari, A.; Mubashir, M.; Asif, S.; Cheah, W.Y.; Manickam, S.; et al. Geospatial Distribution and Health Risk Assessment of Groundwater Contaminated within the Industrial Areas: An Environmental Sustainability Perspective. *Chemosphere* **2022**, *303*, 134749. [CrossRef]

124. Tziritis, E.; Sachsamanoglou, E.; Güler, C. Evaluating Spatiotemporal Groundwater Quality Changes in the Rhodope Coastal Aquifer System (NE Greece) Employing a GIS-Assisted Hybrid Approach of Multivariate Statistics and Inverse Geochemical Modeling. *Sci. Total Environ.* **2024**, *947*, 174676. [CrossRef]

125. Agbasi, J.C.; Ayejoto, D.A.; Egbueri, J.C.; Khan, N.; Abba, S.I.; Ahmad, V.; Abuzinadah, M.F. HERisk and Statistical Clustering Integrated for Health Risk Modelling of PTEs in Natural Water Resources for Drinking and Sanitary Uses. *Toxin Rev.* **2024**, *43*, 513–539. [CrossRef]

126. Vasileiou, E.; Perraki, M.; Stamatis, G.; Gartzos, E. The Effects of Water Rock Interaction and the Human Activities on the Occurrence of Hexavalent Chromium in Waters. The Case Study of the Psachna Basin, Central Euboea, Greece. *EGU Gen. Assem. Conf. Abstr.* **2014**, *16*, 15467.

127. Megremi, I.; Vasilatos, C.; Vassilakis, E.; Economou-Eliopoulos, M. Spatial Diversity of Cr Distribution in Soil and Groundwater Sites in Relation with Land Use Management in a Mediterranean Region: The Case of C. Evia and Assopos-Thiva Basins, Greece. *Sci. Total Environ.* **2019**, *651*, 656–667. [CrossRef] [PubMed]

128. Remoundaki, E.; Vasileiou, E.; Philippou, A.; Perraki, M.; Kousi, P.; Hatzikioseyian, A.; Stamatis, G. Groundwater Deterioration: The Simultaneous Effects of Intense Agricultural Activity and Heavy Metals in Soil. *Procedia Eng.* **2016**, *162*, 545–552. [CrossRef]

129. Pourret, O. On the Emergence of Tortured Phrases: A Threat to Scientific Integrity—The Example of "Heavy Metal". *Eur. Sci. Ed.* **2024**, *50*.

130. Pourret, O.; Hursthouse, A. It's Time to Replace the Term "Heavy Metals" with "Potentially Toxic Elements" When Reporting Environmental Research. *Int. J. Environ. Res. Public Health* **2019**, *16*, 4446. [CrossRef]

131. Pourret, O.; Bollinger, J.C.; Hursthouse, A. Heavy Metal: A Misused Term? *Acta Geochim.* **2021**, *40*, 466–471. [CrossRef]